

# We are IntechOpen, the world's leading publisher of Open Access books Built by scientists, for scientists

6,900

Open access books available

186,000

International authors and editors

200M

Downloads

Our authors are among the

154

Countries delivered to

TOP 1%

most cited scientists

12.2%

Contributors from top 500 universities



WEB OF SCIENCE™

Selection of our books indexed in the Book Citation Index  
in Web of Science™ Core Collection (BKCI)

Interested in publishing with us?  
Contact [book.department@intechopen.com](mailto:book.department@intechopen.com)

Numbers displayed above are based on latest data collected.  
For more information visit [www.intechopen.com](http://www.intechopen.com)



## Some Results on the Study of Kneed Gait Biped

Zhenze Liu<sup>1</sup>, Yantao Tian<sup>1</sup> and Changjiu Zhou<sup>2</sup>

<sup>1</sup>College of Communication Engineering, Jilin University

<sup>2</sup>Advanced Robotic Intelligent Control Center, School of  
Electrical Electronic Engineering, Singapore Polytechnic

<sup>1</sup>China

<sup>2</sup>Singapore

### 1. Introduction

The notion of obtaining passive gaits, powered only by gravity, was pioneered by McGeer[1], who thought that we can perhaps learn about the stability and control of walking by studying un-powered, uncontrolled models.

Some results with McGeer's passive dynamic models of human locomotion suggest that human body parameters such as mass distribution or limb lengths may have more influence on the existence and quality of gait than is generally recognized. The question has been subsequently studied by many other researchers-such as Collins, Garcia and Goswami.

Human locomotion is typically described as having a periodic movement pattern and stable passive gaits were found for both planar and non-planar bipeds on shallow downhill slopes. And the existence of passive limit cycles(periodic behavior) has important implications for the design of walking robots. Some basic definition about the limit cycle has been induced[2][3][6], discrete events, such as contact with the ground, can act to trap the evolving system state within a constrained region of the state space. Therefore, even when the underlying continuous dynamics are unstable, discrete events may induce a stable limit set and limit cycles are often created in this way.

Here the paper will take great interest in the model Goswami presented 1997 and will describe the model geometry, its dynamic parameters, and its governing equations during the swing stage and the transition stage. In addition, a typical walk cycle of the passive robot on a inclined plain with the help of a phase diagram will be discussed, this motion can continue indefinitely due to a delicate balance between the robot's kinetic energy and potential energy. The discussion about the intricate energy transition and also the mutual influence between the swing leg and stance leg will help us to be better aware of the passivity gait of this kind of compass-like biped robot, besides, some further control ideas will be deduced based on this very character thus lead to systematic control design. In spite of this, the paper also present some applicable control strategies on the gait biped to improve its gaits and present some new idea of anti-phase synchronization.

The results of gait biped concluded above can also be extended to the model of three dimensional phase and some useful research results will shed light on new discovery of this terrific field of the gait biped.

## 2. The compass gait biped model

### 2.1 The model description and assumption

The paper will follow the model that Goswami presented in 1997, so called the compass gait biped, shown as Figure 1, is equivalent to a double pendulum with point masse  $m_H$  and  $m$  concentrated at the hip and legs respectively. The leg-length is  $l$ , which is divided into two parts:  $a$  and  $b$ ,  $a$  is the distance from the leg-tip to the position of  $m$  and  $b$  is the distance from  $m$  to the hip center  $m_H$ . The support angle  $\theta_s$  and nonsupport angle  $\theta_{ns}$  determine the configuration of the compass gait. The angle was made by the biped leg with the vertical (counterclockwise positive).  $2\alpha$  is the total angle between the legs, which is defined as the “inter-leg angle”, and in addition is formed during the instant when both legs are touching the ground. The slope of the ground with the horizontal is denoted by the angle  $\phi$

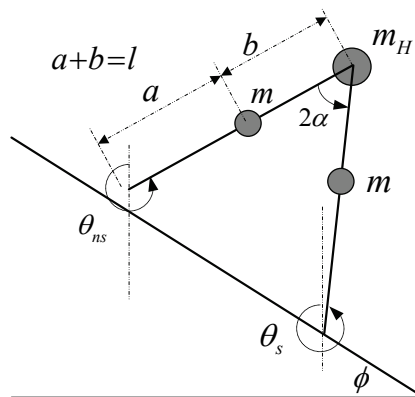


Fig. 1. Model of a compass gait biped robot on a slope

The model has been made by the following assumptions: the total mass of the robot  $m_C = 2m + m_H$  is constant and equal to 20kg. For the sake of simplifying the model, all masses are considered point-masses and the legs are identical with each leg having telescopically retractable knee joint with a mass-less lower leg(shank), this retractable knee joint which is called prismatic-joint knee and is the imaginary concoction, the function of it is to address the conceptual problem of foot-clearance common to all knee-less planar bipeds. The gait consists of swing stage and an instantaneous transition stage: during the swing stage the robot behaves exactly like an inverted planar double pendulum with its support point being analogous to the point of suspension of the pendulum. During the transition stage the support is transferred from one leg to the other. The robot is assumed to move on a horizontal or inclined plane surface. The impact of the swing leg with the ground is assumed to be inelastic and without sliding[4]. This implies that during the instantaneous transition stage the robot configuration remains un-changed, and the angular momentum of the robot about the impacting foot as well as the angular momentum of the pre-impact support leg about the hip are conserved. These conservation laws lead to a discontinuous change in robot velocity.

### 2.2 Dynamics of the swing stage

The dynamic equations of the swing stage are similar to the well-known double pendulum equations. Since the legs of the robot are assumed identical, the equations are similar regardless of the support leg considered.

They have the following form

$$M(q)\ddot{q} + C(q, \dot{q})\dot{q} + g(q) = Bu \quad (1)$$

where  $q = \begin{bmatrix} q_1 \\ q_2 \end{bmatrix} = \begin{bmatrix} \theta_{ms} \\ \theta_s \end{bmatrix}$ ;  $B = \begin{bmatrix} -1 & 0 \\ 1 & 1 \end{bmatrix}$ , and the vector  $u$  represents independent torques at the hip and ankle, which are assumed to be identically zero in the case of passive biped.

The matrices  $M(q)$ ,  $C(q, \dot{q})$ , and  $g(q)$  are given as

$$M(q) = \begin{bmatrix} mb^2 & -mlb \cos(q_2 - q_1) \\ -mlb \cos(q_2 - q_1) & (m_H + m)l^2 + ma^2 \end{bmatrix}$$

$$C(q, \dot{q}) = \begin{bmatrix} 0 & mlb \sin(q_2 - q_1) \dot{q}_2 \\ mlb \sin(q_1 - q_2) \dot{q}_1 & 0 \end{bmatrix}$$

$$g(q) = \begin{bmatrix} mb \sin(q_1) \\ -(m_H l + ma + ml) \sin(q_2) \end{bmatrix}$$

The parameters used for our simulations are  $a = b = 0.5\text{m}$ ,  $l = a + b$ ,  $m_H = 2m = 10\text{kg}$ . Since no dissipation takes place during swing stage, thus the total mechanical energy  $E$  of the robot is conserved during this stage.

### 2.3 Transition equations

The algebraic transition equations relate the robot's states just before and just after its collision with the ground. The support and the non-support legs switch during transition. The pre-impact and post-impact configurations of the robot can be simply related by

$$\theta^+ = J\theta^- \quad (2)$$

With

$$J = \begin{pmatrix} 0 & 1 \\ 1 & 0 \end{pmatrix} \quad (3)$$

The matrix  $J$  exchanges the support and the swing leg angles for the upcoming swing stage. The pre-impact and post-impact variables are identified respectively with the superscripts  $-$  and  $+$ . The conservation of angular momentum principle applied to the robot gives us the following equation

$$Q^-(\alpha)\dot{\theta}^- = Q^+(\alpha)\dot{\theta}^+$$

From which we can write the joint-velocity relationship

$$\dot{\theta}^+ = (Q^+(\alpha))^{-1} Q^-(\alpha) \dot{\theta}^- = H(\alpha) \dot{\theta}^-$$

where

$$Q^-(\alpha) = \begin{bmatrix} (m_H l^2 + 2ml^2) \cos(2\alpha) - mab & & & & \\ \dots - 2mbl \cos(2\alpha) & & & & \\ -mab & & & & \\ -mab & & & & \\ 0 & & & & \end{bmatrix} \quad Q^+(\alpha) = \begin{bmatrix} mb^2 - mbl \cos(2\alpha) & & & & \\ mb^2 & & & & \\ (ml^2 + ma^2 + m_H l^2) - mbl \cos(2\alpha) & & & & \\ -mbl \cos(2\alpha) & & & & \end{bmatrix}$$

With

$$\alpha = \frac{q_1 - q_2}{2}$$

The complete state vector  $q$  before and after impact can thus be written as

$$q^+ = W(\alpha) q^-$$

With

$$W(\alpha) = \begin{pmatrix} J & 0 \\ 0 & H(\alpha) \end{pmatrix}$$

Moreover, it follows with the robot geometry during the transfer

$$\theta_{ns}^- + \theta_s^- = -2\varphi \quad (\text{or } \theta_{ns}^+ + \theta_s^+ = -2\varphi)$$

$$\theta_{ns}^- - \theta_s^- = 2\alpha \quad (\text{or } \theta_s^+ - \theta_{ns}^+ = 2\alpha)$$

where + and - correspond to the instants just after and before the change of support, respectively.

The assumption that the angular momentum of the robot is conserved during the transition doesn't explicitly indicate how the mechanical energy of the robot changes during this stage. we will present a detailed explanation in the following section on the fact that through the transition stage, the change in mechanical energy is always negative.

### 3. Characteristics of steady passive compass gaits

#### 3.1 Description of a typical limit cycle

Due to the hybrid nature[5] of the governing equations, it is impossible to utilize the traditional tool developed to aid the study of this nonlinear systems. McGeer has proposed an idea of linearizing the swing-stage equations of the robot about an equilibrium state, thus making it possible to explicitly integrate these equations. Next the transition equations are concatenated and the conditions for the existence of a periodic solution of this coupled system is found. To study the stability of this periodic solution, a second linearization about

the periodic solution is necessary. The problem with this approach is that the linear solution is valid only within a narrow region around the point of linearization.

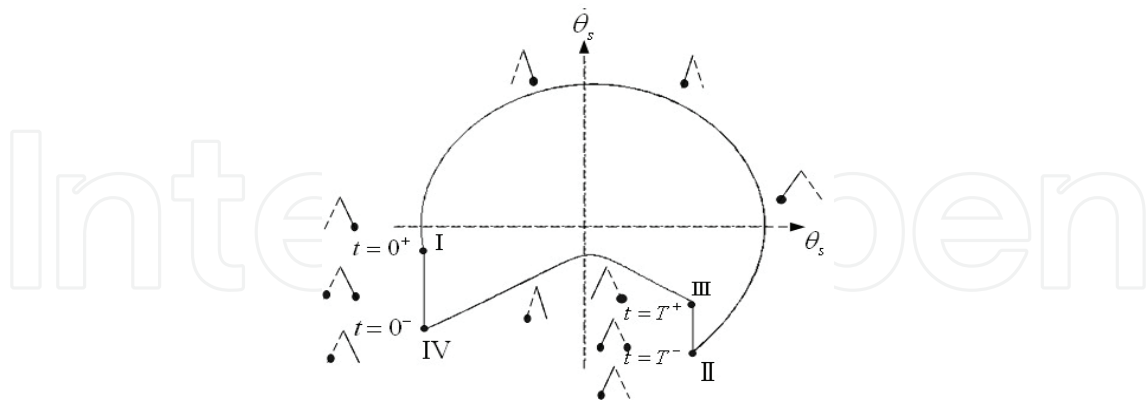


Fig. 2. Phase portrait of a periodic walk. This figure corresponds to only one leg of the biped, one cycle in the figure corresponds to two steps of the robot. In the figure we have indicated some of the time stamps important in the dynamic evolution of the biped. The configuration of the biped has been shown with small stick diagrams. In these diagrams, one leg is dotted, the other leg is solid, and a black dot at the foot indicates the supporting leg.

Figure 2 just presents the sketch of a phase-space limit cycle of a symmetric gait of the robot on a three degree slope.

Follow the phase trajectory at the instant marked I, corresponding to time  $t = 0^+$ , when the rear leg just loses contact with the ground and becomes the swing leg. The phase trajectory evolves in the clockwise sense in the diagram with the cycle from I - II, depicts the swing leg suspended as a simple pendulum from the moving point-hip, at the same time, stance leg "hinged" at the point of support as an inverted simple pendulum. While the swing leg will cross the velocity axis at a positive velocity, the biped is in the vertical configuration. During the process, only the stance leg contacts with the ground, please recall that we have the assumption that there is no slipping at the stance leg ground contact. Instant II corresponds to time  $t = T^-$ , when the swing leg is about to touch the ground. The impact between the swing leg and the ground occurs at the instant  $t = T$ , we observe a velocity jump from II - III due to the impact. In order to simplify the model, we assume that the time during the impact is instantaneous, which means there is an impulse force acting on the biped. Due to this presumption, constant angle momentum is possible and the decrease of the kinetics can be explained by the jump in velocity and inelastic property. At instant III,  $t = T^+$ , the swing leg becomes the support leg and executes the process of III - IV, and it corresponds to the motion of the support "hinged" at the point of support as an inverted simple pendulum. From IV - I, thus  $t = 0^- - t = 0^+$ , the velocity jump appears for another time due to the impact between the current swing leg with the ground, similar to the process II - III, and then the cyclic trajectory is a limit cycle. For the stable gaits, it will attract and absorb all nearby trajectories that enter its attractive basin. This property will be useful for the further control strategy design.

Simulation trials reveal that the passive compass gait robot can walk down a slope with a steady gait. For a given robot, one and only one stable gait on a given slope exists, which symbolize the periodicity of the humanoid gaits, if we can make full use of this property, we

may find some idea on controlling the robots by maintaining the stability of limit cycle through the idea of adding some torque or only adjust the parameter of the system. Moreover, the initial value of the passive walking must correspond with an energy value, for the lost energy during the process of collision should conform to some regulations between the gravity and kinematics. To a certain slope, the limit cycle is the only, so the state point adjoin to the limit cycle can also converge to the limit cycle. The non-linear system possesses the property of being sensitive to the initial value, so the analytical procedure to find this limit cycle still remain a challenge.

### 3.2 The energy analysis in passive gait

Figures 3 depict the variation graph of kinetic energy, potential energy and total mechanical energy corresponding to the limit cycle of certain three slope respectively. Seen from figures, we can clearly specify the whole biped gaits of the robot, the kinetic energy (KE) and the potential energy (PE) have a complex variation process just not as we have expected before. KE just experiences an asymmetry periodic process. At instant  $T$ , a sharp downwards jump exists because of the inelastic impact of the legs and the ground thus causing the loss of the kinetic energy dramatically, we can clearly see from Figure 3 that the reduction of the energy is irregular just due to the inertial kinetic energy compensation of the stance leg, the enhancement of kinetic energy is partly compensated by gravity, the detailed message of the variation of the energy and conversion can be informed in figures. While PE just experiences a contrary process. During the swing stage, gravity and only gravity acts on the robot, so the whole mechanical energy of the system will keep constant. At instant  $t = T$ , mechanical energy will also have a downward jump, this variation value will be equal to the kinetics'. The potential energy decreases continuously during the whole process, we can tell from figures that some coupling phenomenon exists between the swing leg and the stance leg, similar to that 2-dof mechanical configuration. Mutual influence between the two legs can be observed indirectly by figures and also will help us in realizing this complex hybrid system.

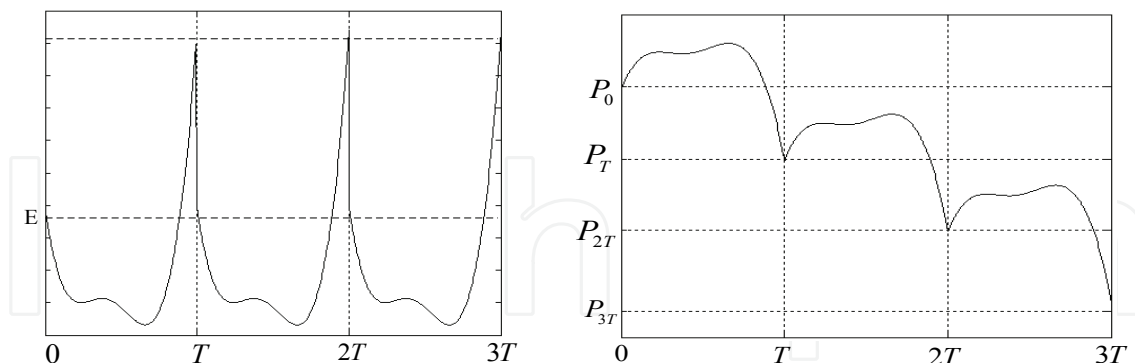


Fig. 3. The kinetic energy and potential energy variation graph corresponding to the limit cycle of certain three slope

Seen from Figures, we present the variation and comparison graph. And some important points  $t_0, t_1, t_2, t_3, t_4$  have been selected out to explain the whole biped gaits, they represent the instant corresponding to different culmination points during the steady gaits period. During the whole walking course, KE and PE curve just go along with the direction  $t_0 - t_1 - t_2 - t_3 - t_4$ , amid of it,  $t_0 = 0$ ,  $t_4 = T$ . The graph can tell us some details about the particular energy variation of the whole steady robot gaits.

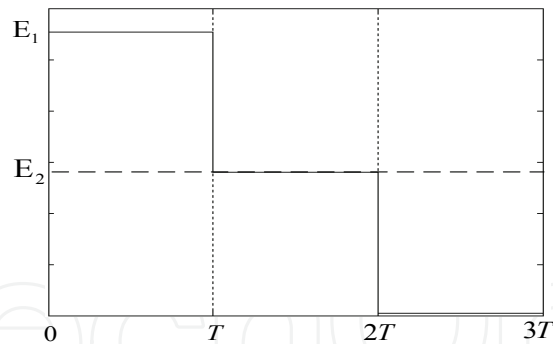


Fig. 4. The total mechanical energy variation graph corresponding to the limit cycle of certain three slope

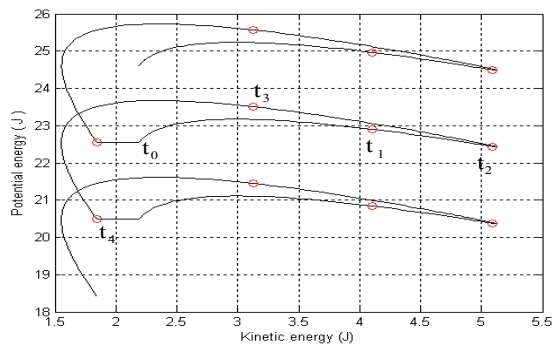


Fig. 5. The variation and comparison graph of KE and PE conversion of the swing leg during steady robot gaits of certain 3 degree slope

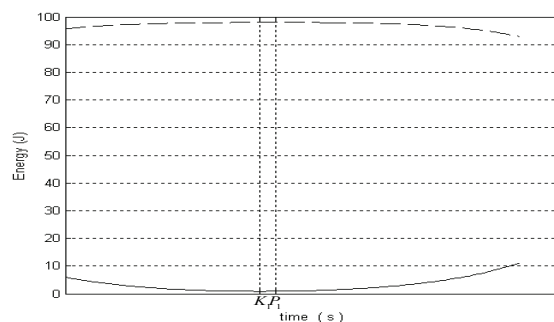


Fig. 6. The graph on the two nearest existed culmination values of KE and PE corresponding to the course of energy conversion of the swing leg within one gait cycle

Seen from Figures we address the culmination values corresponding to the course of energy conversion. There are three culmination points of KE and two culmination points of PE within one steady gait period. For Figure 11, we can set the culmination potential value of the swing leg as  $P_1, P_2, P_3$  from the left to right, and also set two culmination kinetic value of the swing leg as  $K_1, K_2$  with the same sequence above within one gait cycle, the maximum and minimum of the energy can be observed. The figure just search out the culmination point of the two nearest point as  $k$  and  $p$ , the potential energy culmination point just drop behind the kinetic energy culmination point even they are adjacent while

they are not the same point as we had thought before. The reason will be well explained in the following section.

Theoretical speaking, the mechanic energy should keep constant during the swing stage corresponding to the stable walking limit cycle. Virtually, total mechanic energy will decrease incessantly during the swing stage. While the reduction of the magnitude can be omitted comparing with total energy magnitude. The reason that we mention this problem is that due to the complexity of the non-linear system, it is necessary to make some adjustments sometimes in order to get the better results when considering the control strategy of the system.

The phenomena called “rub ground” will exist during the swing stage, this phenomena just happens at the time before the superposition of two legs and ends just at the instant of the superposition of two legs. The height between the swing leg and the ground will be negative when the swing leg swings from the start to the vertical position by simulation results corresponding to steady robot gaits of certain 3 degree slope, the maximum of the height will reach  $-0.0033\text{m}$ . Why this phenomenon exist and how to avoid this state which we intuitively sense unrealistic? We can solve this problem by some technique methods such as the assumption discussed in the second part of the paper- the introduction of a purely imaginary concoction so called prismatic joint knee. The prismatic joint is assumed to retract the lower leg to clear the ground, and the retraction of the lower leg is assumed mass-less, it will not affect the robot dynamics and the swing leg returns to its original length  $l$  at transition. The assumption is very necessary for the existence of the limit cycle and many properties of the bipedal gaits can be observed directly and also will guide us in some directions: for example, what is the relationship between the point of intersection of two legs and the height between the swing leg and the ground? For real gaits of the robot, we can modify the value of the graph to keep tracing the steady gaits of the robot.

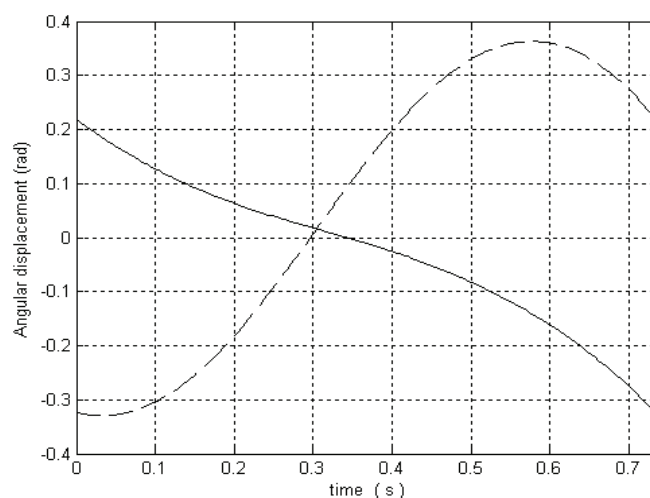


Fig. 7. The relationship graph of angle position between the swing leg and the stance leg ‘---’ just represents the swing leg and ‘—’ just represents the stance leg, the same with the following figures.

Seen from Figure 15, the angle position curve of the swing leg is much more approach to sine wave, while the stance leg has a comparative big difference with the swing leg. This can be explained that the stance leg experiences a compelled motion, with the action force

coming from the swing leg as well as gravity. And in addition, the coupling degree of the two legs vary at different instant.

The angle position will be more than zero when two legs are in the state of superposition, which means the joint of superposition lies in the left side of the vertical direction. When the swing leg becomes straight, the angle of the stance leg will be positive, and the stance leg the same.

Here the focus of the work is a relative further study of the passive gait of a compass-like, planar, biped robot on inclined slopes, an analysis about the distribution of the energy and also the conversion law between the swing leg and the stance leg during the process of the steady robot gaits, have been discussed in the paper. Phase-position property corresponds to the limit cycle, the coupling properties between two legs, the existence of the culmination points which produced in the course of the conversion of KE and PE are also the topic of the research. To a certain slope angle  $\phi$ , one and only one stable limit cycle exists.

The research of the paper will have positive significance in getting better aware of the law and global property to biped gaits of the robot. The model we adopt here is an ideal position, how to induce or modify a more realistic model for biped gaits, and how to enlarge the initial value attraction region of the limit cycle as well as how to apply the efficient control on the robot combined with its own property with the least energy possible will guide our further research direction.

#### 4. Some simple control laws

The existence of passive gaits in simple bipeds is interesting and may help to explain the efficiency of human locomotion. In particular, the sensitivity to initial conditions and ground slope must first be emphasized [8]. In spite of this, robustness to external disturbances and parameter uncertainty must be investigated. In the paper, we address simple control law for the compass gait biped by tracking a given mechanical energy of the robot with the torque added on the hip and ankle respectively.

##### 4.1 The idea of control law tracking passive energy level

As the robot walks down on a slope, its support point also shifts downward at every touchdown, the kinetic energy will increase accordingly as it loses gravitational potential energy. In a steady walk, at the end of each step by the impact, the amount of kinetic energy will absorb the loss of the gravitational potential energy. This character presents us an idea on control passive biped robot, if, at every touchdown we reset our potential energy reference line to the point of touchdown, then the total energy of the robot appears constant regardless of its downward descent. We name the characteristic energy of the passive limit cycle on a given slope as "reference energy", the function of it is to drive the robot toward it thus attain to a mobile balance.

The approach assumes that we have already identified the passive limit cycle for a given slope and the advantage of it is that it is able to generate gaits which don't exist for the unpowered robot. In addition, at the same time, only those neighborhoods of the passive gait can function well by this control law. The total mechanical energy  $E$  of the robot can be

expressed as  $E = 0.5 \dot{\theta}^T M \dot{\theta} + PE$ . The power input to the system is the time rate of change of the total energy,  $\dot{E} = \dot{\theta}^T B u$  for a passive cycle  $u = 0$ , and the reference energy of the limit cycle is

$E^* = E(\dot{\theta}^*, \theta^*)$ . Here we use a simple damper control law of the form  $Bu = -\beta \dot{\theta}$ . So the power input to the system is therefore  $\dot{E} = -\dot{\theta}^T \beta \dot{\theta}$ . For a positive definite  $\beta$ , the quantity  $-\dot{\theta}^T \beta \dot{\theta} < 0$ , which means that the robot's kinetic energy decreases monotonically. In order to simplify the choice, we can further specify that the control law should bring the current level of the robot to the reference energy level at an exponential rate. Three ways of the control law[9] will be implemented: by means of the two actuators acting independently or them acting together on the hip or in the supporting leg at the point of support, the latter will be also called as "support ankle torque". The paper will have a discussion about the latter two control strategies.

#### 4.2 Control with hip torque

We propose a control law of the following form based on the idea presenting above then after the calculation we get

$$u_H = -\frac{\lambda(E - E^*)}{\dot{\theta}_s - \dot{\theta}_{ns}} \quad (4)$$

$\lambda$  is a parameter influencing the degree about the rate of convergent to the reference energy level. At the state of  $\theta_s - \theta_{ns} = 0$ , the control law will have a singularity, to solve this problem, the common idea is to set the control to zero whenever  $\|\dot{\theta}_s - \dot{\theta}_{ns}\| < \varepsilon$ . To the passive limit cycle on a  $3^\circ$  slope, we make some active phase cycle superimposed on it, and from the picture, we let the starting position, denote as A, lie outside the basin of the attraction of the passive limit cycle. In this situation the passive robot would have fallen down soon, while the control law will lead the gait of the robot go back into the state of limit cycle and thus keep the periodic state. We can come to the conclusion from the control that the basin of attraction of the passive limit cycle has been enlarged and this will have a realistic sense in the application of the further study.

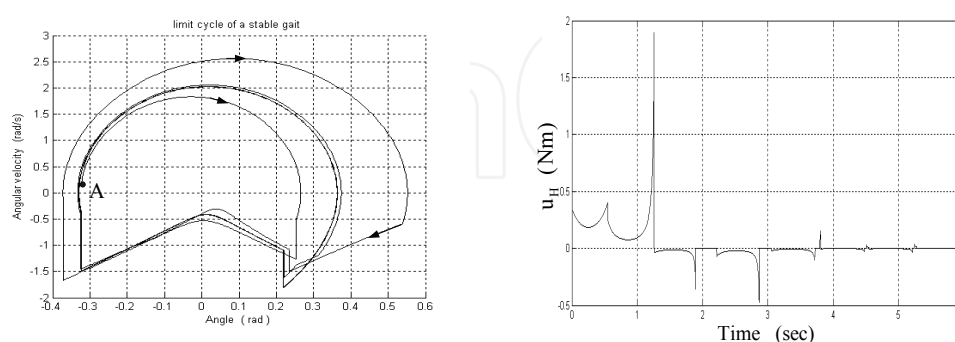


Fig. 8. Active stabilization of a limit cycle. Here we show the performance of the energy tracking law for a robot walking down a  $3^\circ$  slope. The system driven only by a hip torque seeks and returns to the passive cycle of the robot. The initial condition is denoted as point A, lying outside the basin of attraction of the passive limit cycle. Through the control strategy, the system has been brought back to the limit cycle. The right will be the graph of the variation graph on the control added on the hip

Seen from Figure, we conclude that the system will run away from the limit cycle without the added control. While added with control, the system will make a 3-4 gaits adjustment to converge to the original limit cycle and then keep its stable gait state, which proves the validity of the control. Figure 4 just depicts the variation on total energy based on the hip control condition, we can clearly see that the total energy will fluctuate within a transitory process and then go into a constant value which corresponding to the energy of the limit cycle. From Figure, we can explicitly be aware of the detailed variation on the control torque act of the hip and of the every gait state. To seek for the deep relationship between the variations of added torque, the variation regulation of the energy control and also the property of the limit cycle will be useful.

Then, we observe the process with the starting position lying inside the basin of attraction of the passive limit cycle of certain slope (here  $3^\circ$ ).

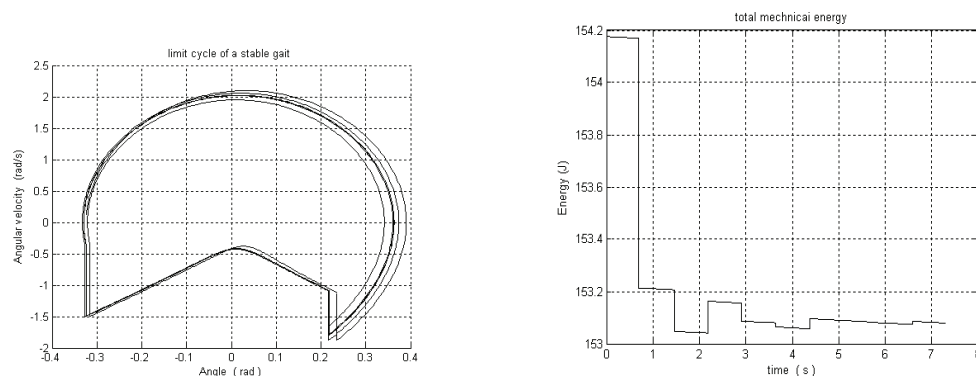


Fig. 9. Limit cycle corresponding to the certain three slope with the initial condition lying in the limit cycle The variation on total energy corresponding to the condition as Figure has demonstrated.

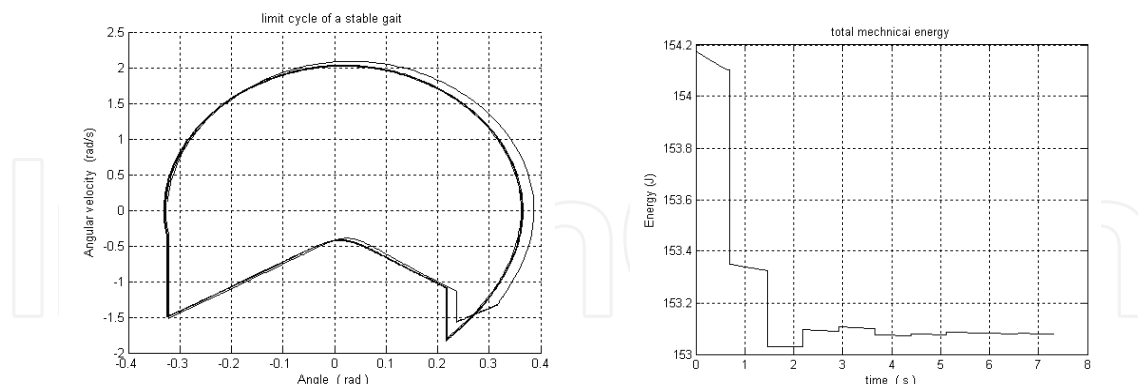


Fig. 10. Limit cycle with hip control corresponding to the condition as Figure And the variation on total energy corresponding to the condition as Figure 8 has demonstrated.

Figures 9 and 10 just show us something about the limit cycle corresponding the certain three slope with the initial condition lying in the limit cycle and also the variation of total mechanical energy corresponding that condition.

Figures 9 and 10 just show us the whole process with control added on the hip. Seen from the picture, we may safely find that time consuming in going into the limit cycle has been improved a lot evidently, with only two gaits the gait will converge to its stable period with

control comparing at least 4 gaits to the same limit cycle by its own convergence. The variation on the total mechanical energy just describes the whole process of the biped gaits. In another words, with the control on the hip we may efficiently improve the quality of the convergence of the passive limit cycle.

Next, we'd meant to make unnatural limit cycles to track the certain target mechanical energy denoted by  $E^{tar}$ , which is different from the reference energy corresponding to that slope.

By the use of hip control, we can successfully produce new gaits, while it is very interest for us to see that the consequence in tracking the specified target energy can not match the very exact result that we expect, it will converge to the energy cycle which is adjacent to the target energy cycle. That is to say, the control strategy can help us to track any appointed target energy in some degree and will guide us to get better aware of the property of the passive gait control.

$$E^{tar} = 156J$$

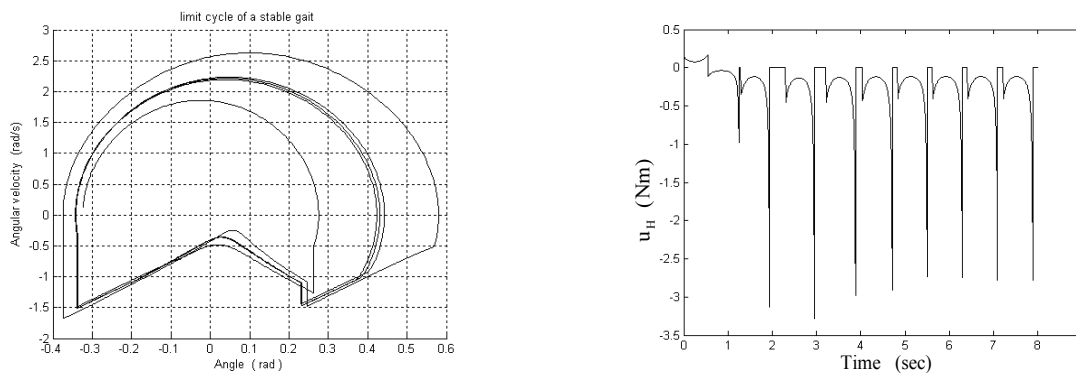


Fig. 11. Target energy tracking control and also the variation graph by using hip actuator on the control added on the hip

The target energy we'd like to track	The final attained energy with hip control
$E^{tar} = 154J$	$E^{final} = 153.1348J$
$E^{tar} = 156J$	$E^{final} = 153.1520J$
$E^{tar} = 158J$	$E^{final} = 153.1480J$
$E^{tar} = 160J$	$E^{final} = 153.1088J$

Table 1. The relationship between active biped gait for different target energies and the energy level at which the robot converged at the end.

Seen from Table 1, we find that no cycle with an energy level  $E^{tar}$  less than that corresponding to the passive cycle could be generated

#### 4.3 Control with ankle torque

We will implement the same control law employing only the support ankle torque following the above hip control, and then we have:

$$u_s = -\frac{\lambda(E - E^*)}{\dot{\theta}_s} \quad (5)$$

With the same procedure depicted as section 3.2, to the passive limit cycle on a  $3^\circ$  slope, we make some active phase cycle superimposed on it, we let the starting position, denote as A lie outside the basin of the attraction of the passive limit cycle, and in this situation the passive robot would have fallen down soon. While the control law will make the gait go into the state of limit cycle and thus enlarge the basin of attraction of the passive limit cycle.

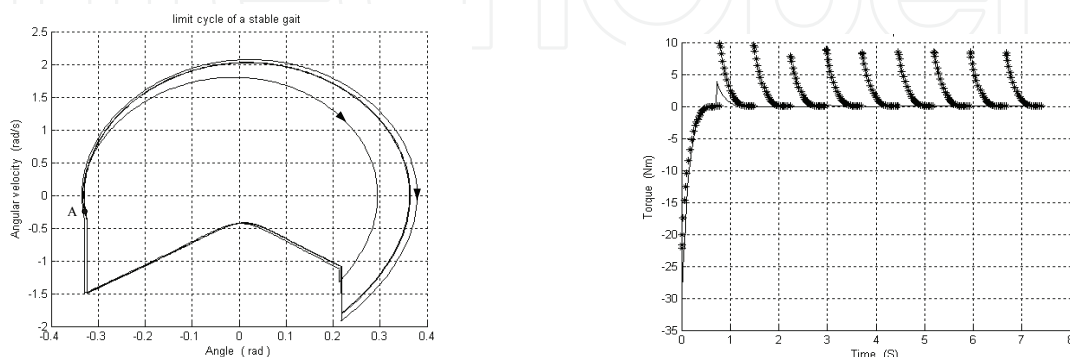


Fig. 12. Active stabilization of a limit cycle. Here we show the performance of the energy tracking law for a robot walking down a  $3^\circ$  slope. The system driven only by an ankle torque on the stance leg seeks and returns to the passive cycle of the robot. The initial condition is denoted as point A, lying outside the basin of attraction of the passive limit cycle. Through the control strategy, the system has been brought back to the limit cycle. And the right one will be the Energy tracking control using support ankle actuation. Ten steps of the robot are presented here. The support ankle alternates between the left and the right ankle. The black dot represents the energy  $E_{tar}=152.6\text{J}$  and the real line represents the energy  $E_{tar}=153.08\text{J}$ .

Figure 12 reveals the evolution of ankle torque. The repeated peaks in the control torque correspond to the time instants of foot touchdown. The zero of the time axis in the figure represents the beginning of a swing stage. Seen from this Figure, control is active from the beginning and as the robot's energy reaches the reference energy, the control becomes zero, clearly, foot touchdown has caused a sudden change in the angular velocity and also the system energy. In reality, arbitrarily large torques can't be applied as it may cause the robot foot to roll on the ground or maybe leave the ground.

We can come to a conclusion from Figure 16 that the target energy that we appoint ahead must lie in a relatively narrow region in order not to run away from the stable periodic state due to the property of non-linear system. We have found during the study that if we choose the target energy a little farther away from the reference energy, with only ankle control, the target energy that we expected can't be tracked successfully. Seen from Figure, the total energy will never converge to a constant value as we expect. Figure 12 below just address the region about limit cycle of a stable gait with ankle control in certain slope.

For the study to the ankle torque control and the hip torque control, we come to the result that the main difference between them, is that for the hip control discussed above, we can effectively converge to any target energy (within a limit), which has much larger region than the ankle control. The reason will be explained as the ankle control is capable of more

directly affecting the overall dynamics of the robot. Whether controlled at the hip or at the ankle, the control law will enlarge the basin of attraction of the limit cycle.

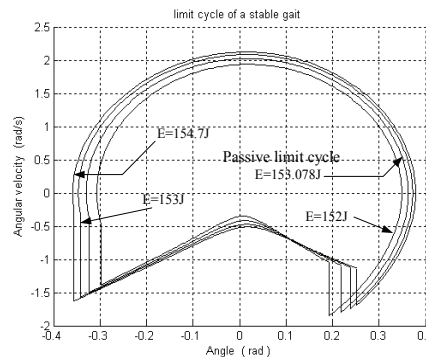


Fig. 13. Some region about limit cycle of a stable gait with ankle control in certain slope

In addition, we will pay more attention to the study about two actuators added at the hip and ankle together in the future work and it will be useful to identify the boundary of the basin of attraction and to determine the favorable initial conditions. In spite of all stated above, we should also know that the robot's behavior is heavily influenced by the impact model which is not the only available impact model, how to model some new realistic foot/ground impact models possessing such a manner that reasonable perturbations of the model parameters don't dramatically change the gait, should be considered.

## 5. The complicated idea of controlling the gait biped with energy based control slope invariance law

### 5.1 Controlled symmetry and slope invariance

The idea that passive limit cycles can be made slope invariant by a control that compensates the gravitational torques acting on the biped has been proposed by Mark. Spang.

The result just relies on some symmetry properties in the Lagrangian dynamics of robots with respect to rotations of inertial frame. A group action of  $SO(n)$  has been defined to change the ground slope with respect to the inertial frame on  $Q$ , for  $n=2$  in the planar case, this group action takes a particularly simple form as

$$A = \begin{bmatrix} \cos \varphi & -\sin \varphi \\ \sin \varphi & \cos \varphi \end{bmatrix} \in SO(2) \quad (6)$$

The group action,  $\phi_A: Q \rightarrow Q$  is given by

$$\phi_A(q) = (q_1 + \varphi, q_2 + \varphi) \quad (7)$$

The so called lifted action on  $TQ$  is

$$(\phi_A(q), T_q \phi_A(\dot{q})) = (\phi_A(q), \dot{q}) \quad (8)$$

The kinetic energy and impact equations are invariant under this group action and if  $q(t)$ ,  $\dot{q}_i(t)$  is a solution trajectory of (1), with  $u = 0$  then  $\phi_A(q)$ ,  $\dot{q}$  is a solution of

$$M(q)\ddot{q} + C(q, \dot{q})\dot{q} + g(\phi_A(q)) = 0 \quad (9)$$

Via the control

$$u = B^{-1}(g(q) - g(\phi_A(q))) \quad (10)$$

The limit cycle of Figure can be reproduced on any ground slope via active control that effectively cancels the gravity vector that corresponds to the current slope.

## 5.2 Energy based control to the gravity compensation control

Using this gravity compensation control of the previous section. We let

$$u = B^{-1}(g(q) - g(\phi_A(q))) + \bar{u}$$

So that (1) becomes

$$M(q)\ddot{q} + C(q, \dot{q})\dot{q} + g(\phi_A(q)) = B\bar{u}$$

The design of the additional term  $\bar{u}$  is to increase the robustness to slope variations. Set  $S$  as a storage function

$$S = \frac{1}{2}(E - E_{ref})^2 \quad (11)$$

$E$  is the total (kinetic and potential) energy

$$E = \frac{1}{2} \dot{q}^T M(q) \dot{q} + V(q)$$

And  $E_{ref}$  is the constant energy of the biped along the limit cycle trajectory of the system corresponding to a fixed ground slope. A simple calculation shows that

$$\begin{aligned} \dot{S} &= (E - E_{ref}) \dot{E} \\ &= (E - E_{ref}) \dot{q}^T B \bar{u} \end{aligned}$$

Where the second equality comes from the usual passivity or skew-symmetry property of rigid robots. Based on the above deduction, we design the following control scheme

$$\bar{u} = -kB^{-1}(E - E_{ref})\dot{q} \quad (12)$$

Where  $k$  is a scalar gain, and we can easily get the results as

$$\dot{S} = -2k \left\| \dot{q} \right\|^2 S \leq 0 \quad (13)$$

So the function  $S$  works just as a Lyapunov function. Thus the total energy of the biped will thus converge exponentially toward the reference between impacts. At the impact the storage function will exhibit a jump discontinuity. It follows from standard results in hybrid system theory that, if less than its value at the previous jump, then the total energy will converge asymptotically to the reference energy as  $t \rightarrow \infty$ .

### 5.3 Some results with energy tracking

Figures in this section will show that the addition of the total energy shaping control  $u$  results in both an increase in the basin of attraction of the limit cycle and increased convergence to the limit cycle. This has important consequences for robustness to external disturbances as well as uncertainty and variations in the ground slope.

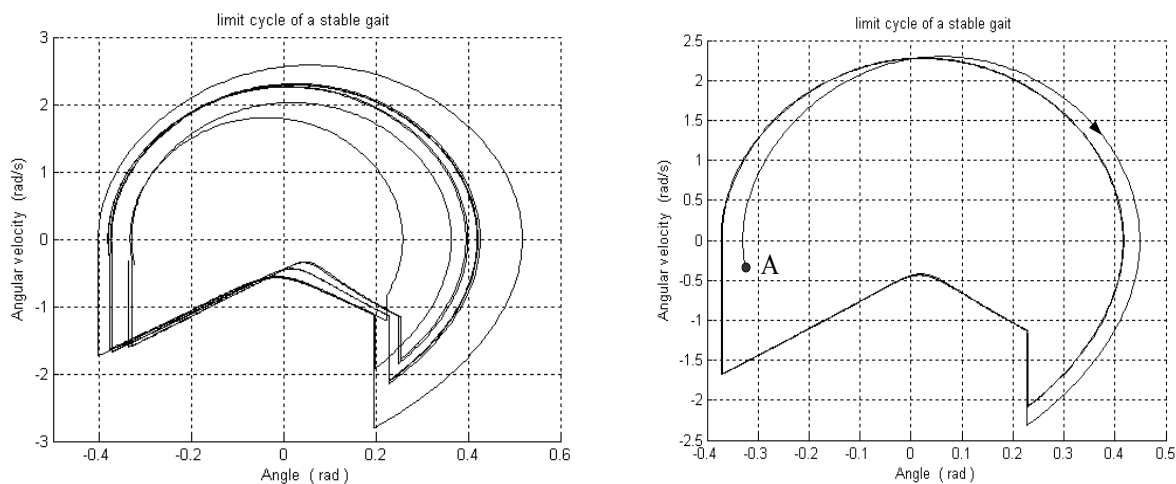


Fig. 14. Convergence to the limit cycle (a) without total energy control (b) with total energy control

With total energy control, the biped trajectory converges to the limit cycle in one to three steps depending on the initial conditions whereas without the total energy control convergence is much slower, on the order of ten to twelve steps just as Figure 3 shows. And Figure just presents the variation process with the energy explanation variation graph. The whole detailed convergence process will be identified in the figure. The value of the storage function,  $S$ , shown in Figure 14, will decrease at each step, the implication of this is that the trajectory after each step moves closer to the limit cycle on which the energy equals the reference energy.

Seen from figure 14 (a), the initial condition lies outside the region to the limit cycle, and the robot will fall down with asymmetry gaits under this condition. By the idea of control, the trajectory of the gait will be brought back to the stable limit cycle only within few steps, this proves that, with control, an increase occur in the basin of attraction of the limit cycle.

The convergence speed and convergence efficiency of the control will be influenced by scalar  $k$  in great degree. With the simulation, a result comes out that it is not right for  $k$  to be the larger the better, virtually this feedback coefficient will possess a more complex variation during the whole control process. That is to say, there exists an "optimal" choice as well as appropriate value for  $k$  beyond which the stability is degraded, the choose value of this  $k$  will be preferable important for the control of the limit cycle.

#### 5.4 Slope variation

As a further illustration, the performance of the system when the slope exhibits a sudden change will be presented. The control input is determined by the local slope, which is the ground slope at the stance leg. The local slope can be determined by the two-point contact condition which occurs at the moment of contact of the swing foot with the ground thus for a discrete slope change. Figure 8(a) shows that, without the total energy control, the robot is not able to maintain a stable gait. Figure 8(b) shows that, with the addition of the total energy based control  $\bar{u}$ , the biped successfully makes the transition between slopes. During the course of simulation, we can come to the conclusion that  $E_{ref}$  will be the decisive factor to the control, and it must correspond to certain angle  $\phi$ , otherwise the control strategy will be out of function.

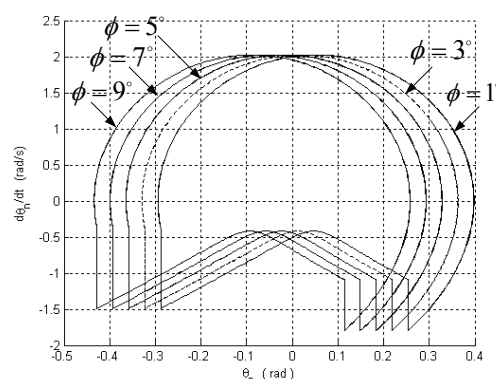


Fig. 15. The limit cycle corresponding to different slope angle using the control  $\bar{u}$  with  $\phi_0 = 3^\circ$

Figure 15 just addresses the detail for the limit cycle corresponding to different slope angle using the control  $\bar{u}$  with the initial  $\phi_0 = 3^\circ$ . The control idea is thus to make the robot vary at different limit cycle to keep stable walking gaits when facing different suddenly slope change and in addition this control idea is shown to be effective in generating new stable walking gaits for biped robots. Definitely the total energy control increases the basin of attraction but there are still limits to the range of slope variation as well as disturbances that the biped can tolerate. Increasing the basin of attraction further would improve the applicability of these passivity based ideas.

#### 6. Control of average progression speed with two actuators

Energy based control slope invariance law just discussed above works pretty well in some occasion while the law neglects the truth that actually the speed of walking gaits should be considered in some degree in passive walking when creating steady gaits. In order to solve the problem, so called average progression speed control strategy which Goswami has proposed will help us to establish the relationship between the average speed of progression and the target energy to improve the robot performance.

This control strategy for the robot is on the basis of the principle that the total energy of robot appeared constant regardless of its downward descent. The control law tries to drive the robot toward the reference energy corresponding to the energy of the limit cycle on given slope. The assumption is that, for the given slope, a passive limit cycle exists and have

already been identified. Although this may appear extremely constraining at first, while the advantage is that gaits can be generated which don't exist for the un-powered robot.

The total mechanical energy  $E$  of the robot can be expressed as  $E = 0.5\dot{\theta}^T M \dot{\theta} + PE$ . The power input to the system is the time rate of change of the total energy,  $\dot{E} = \dot{\theta}^T S u$ , for a passive cycle  $u = 0$  and the reference energy  $E^* = E(\theta^*, \dot{\theta}^*)$ . A simple damper control law of the form  $S u = -\beta \dot{\theta}$  is used here. The power input to the system is therefore  $\dot{E} = -\dot{\theta}^T \beta \dot{\theta}$ . For a positive definite  $\beta$  the quantity  $-\dot{\theta}^T \beta \dot{\theta} < 0$ , which means that the robot's kinetic energy decreases monotonically. In order to simplify the choice, specify that the control law should attempt to bring the current level of the robot to the reference energy level at an exponential rate.

The hip actuator and the actuator in the supporting leg at the support of leg are available at any instant. This section will have a study on the performance of the control law with both actuators.

### 6.1 Control of two actuators

The idea on the control of average progression speed will be discussed as the following. The average speed per step is given by  $v = \frac{2l \sin \alpha}{T}$ , the  $k^{\text{th}}$  step target energy is  $E_k^{\text{tar}}$ , which is equal to that the  $k-1^{\text{th}}$  step with an added term. And this target energy is proportional to the error in speed.  $E_k^{\text{tar}}$  is expressed as

$$E_k^{\text{tar}} = E_{k-1}^{\text{tar}} + \eta(v^{\text{tar}} - v_{k-1}) \quad (14)$$

$\eta$  is a weighting factor between energy and speed. A simplification is obtained by imposing that the hip torque be proportional to the ankle torque with a proportionality constant of  $\mu$ , thus  $\mu = [1 \quad \mu]^T \mu_H$ , while the relationship of the actuator between hip torque and ankle torque can be assigned at any rate that we expect.

$$\mu_H = \left\{ \begin{array}{ll} \frac{-\lambda(E - E_k^{\text{tar}})}{\dot{\theta}_s(1 + \mu) - \dot{\theta}_n} & \text{if } \left\| \dot{\theta}_s(1 + \mu) - \dot{\theta}_n \right\| > \varepsilon \\ 0 & \text{otherwise} \end{array} \right\}$$

With the implementation of the control law corresponding to two actuators, some satisfactory control results have been acquired and the strategy has been proved to be valid in tracking reference energy considering the influence of speed.

Figures 16 will show us some detailed message about the process that through the two actuators control in tracking the limit cycle. It will just take the robot about 30-40 gaits to walk into the limit cycle that we appoint. The collision with the ground is avoided by means of the retraction of the mass-less shank of the swing leg. In general, if the inclination of the upward slope is increased, the robot tends to lengthen the step length in order to maintain the specified speed. The same control law can be easily extended to control the robot on a terrain with a series of plane surfaces with changing slopes.

As shown in Figures 17, the desired speed is reached for a large range of values of  $\lambda$ . As the target speed is less than that corresponding to the passive limit cycle, the robot tries to lengthen its step length and the step period to maintain a constant average speed.

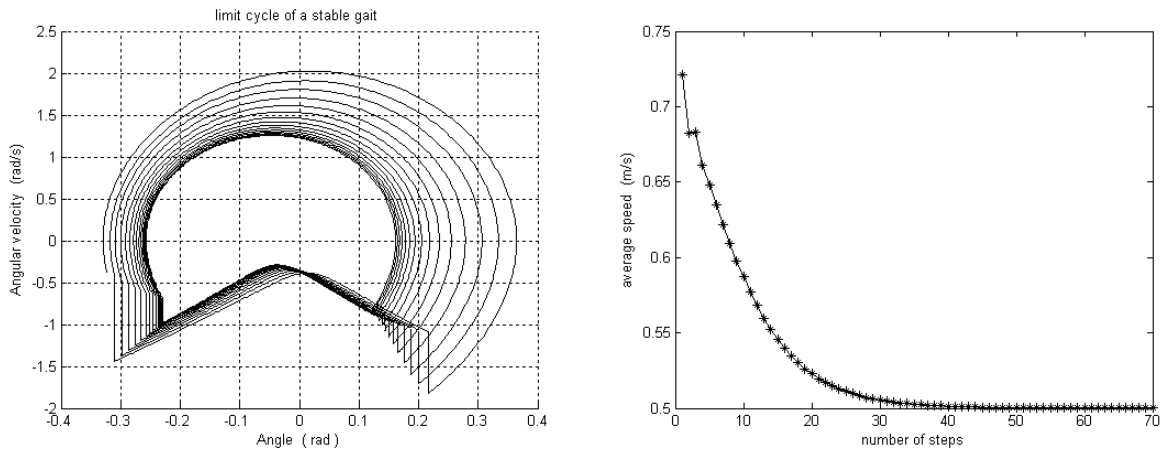


Fig. 16. Phase plane representation of the energy tracking control with two actuators added on the hip and the ankle together. The right will be the average speed and the number of steps corresponding to the two actuators control

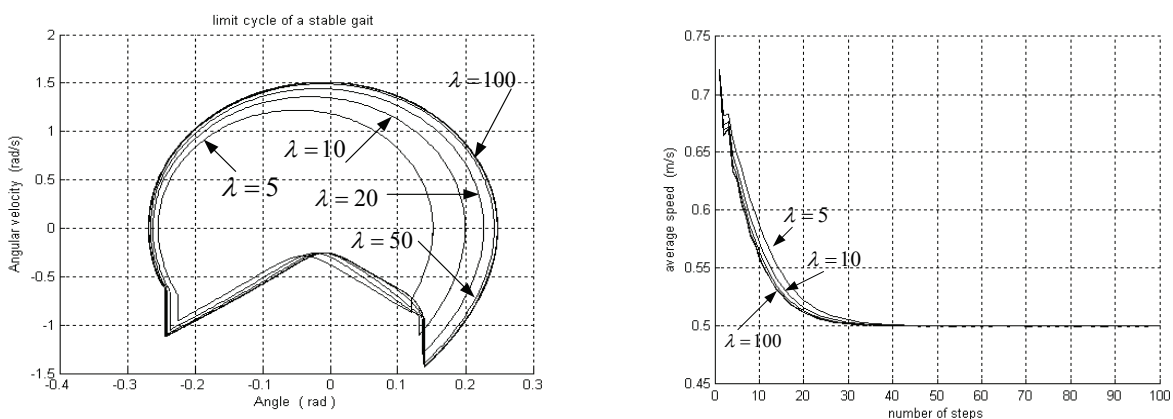


Fig. 17. Phase plane representation of the energy tracking control with respect to the different parameter  $\lambda$  using two actuators. The average speed and the number of steps with respect to the different parameter  $\lambda$  using two actuators

**6.2 Some discussion about parameter variation**

With the control, we find that the average progression speed control strategy can works pretty well in solving some more difficult walking gait with the appropriate parameter variation. Control of the average speed with two actuators ensures the convergence to an active cycle for a reasonably specified speed. The control law has been studied in detail by changing one parameter at a time while holding the others fixed. The parameters concerned are  $\lambda, \mu, \eta, E_0^{tar}$ . The following simulations are carried with for the following parameter as

$$\phi = 0.0524, \alpha = 0.2710, E_{ref} = 153J,$$

$$\lambda = 5, \mu = 5, \eta = 2, V_{tar} = 5m / s.$$

$\lambda$	The desired average speed is reached for a large range of values of $\lambda$
$\mu$	For higher values of $\mu$ , it will cause a bifurcation leading to asymmetric or 2-periodic gaits. In such a gait the average speed oscillates around the target speed, the amplitude of this oscillation increases with $\mu$
$\eta$	Will slightly affect the speed of convergence to the cycle. And when it is zero the target energy is not updated at every step so for a target energy equal to the reference energy the robot converges to the passive limit cycle.
$E_0^{tar}$	Affects the rate of convergence to the target speed. The target energy is modified at every step and we can't predict a priority to what final energy the robot will converge.

Table 1. Effect of  $\lambda$ ,  $\mu$ ,  $\eta$ ,  $E_0^{tar}$ 

$\mu$	$\alpha(^{\circ})$	$v(m/s)$	$T(s)$	$E_{final}(J)$
5	9.9240	0.5	0.6890	148.9767
8	10.5769	0.5	0.7339	149.2529
10	10.8739 and 10.4443	0.5222 and 0.4778	0.7222 and 0.7584	149.8433 and 149.9025

Table 2. Effect of  $\mu$  on the control performance. The table corresponds to simulations on a  $3^{\circ}$  slope with parameters:  $\lambda = 5$ ,  $E^{tar} = 153 J$ ,  $\eta = 5$ 

The most curious effect of  $\mu$  is that for higher values, it will cause a bifurcation leading to asymmetry or 2-periodic gaits just shown as the data of Table 2. In such a gait, the average speed oscillates around the target speed, and the amplitude of this oscillation increase with  $\mu$ . And figure 15 will show us the limit cycle under the so called 2-periodic gaits state. At this time, the gaits just locate in the limit cycle and is about to get away from this stable state if some slight disturbances working on the gaits. In addition, when getting out of this state, the walking gait of the robot will go into chaos and then slip down. Figure 16 is the graph of the average speed and the number of steps with 2-periodic gaits state. With different initial energy value, the graph of average speed and the number of steps will be different due to the sensitivity of chaos.

Furthermore, some more attention should be paid to the work of how to identify the boundary of the basin of attraction and how to determine the favorable initial conditions effectively. In spite of all those stated in the paper, there still exists some other problems such as the robot's behavior is heavily influenced by the impact model which the paper proposed is not the only available impact model. How to model some new realistic foot/ground impact models possessing such a manner that reasonable perturbations of the model parameters don't dramatically change the gait, should be considered.

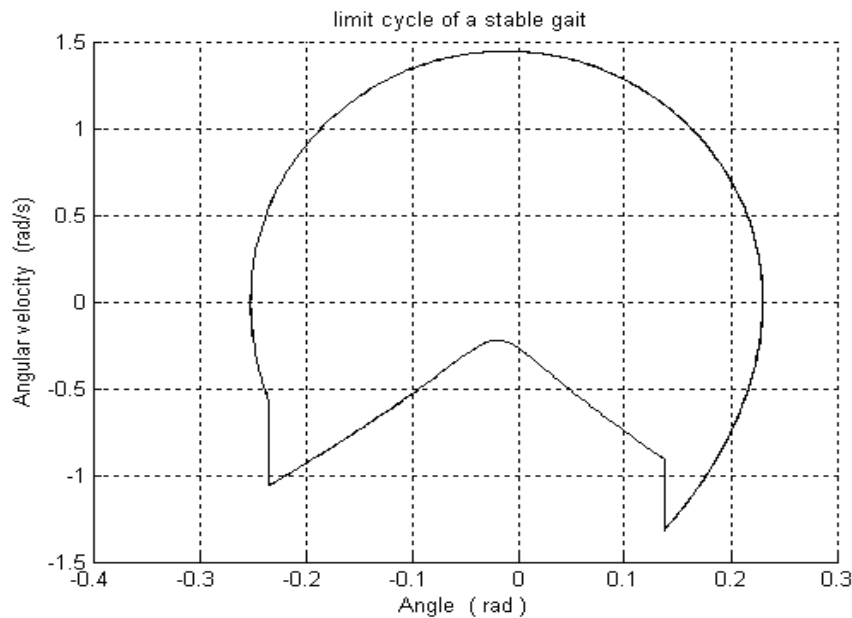


Fig. 18. Phase plane representation of the energy tracking control using two actuators with 2-periodic gaits state.

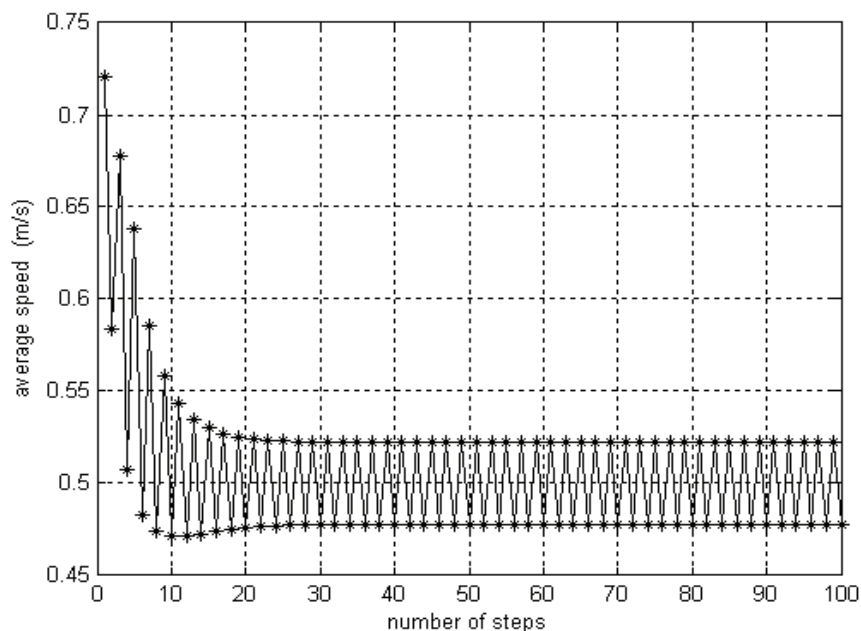


Fig. 19. The average speed and the number of steps corresponding to the two actuators control with 2-periodic gaits state

## 7. Influence of robot parameters on the gait

This section presents the effects of continuous change of the parameters  $\phi$ ,  $\mu$  and  $\beta$  on the gait of our compass-like biped robot. First we discuss the limitations of a linear model in predicting the robot's long term behavior. Next we point out the general features of the

symmetric gaits of the robot-this section mainly consists of a graphical presentation. When one of the parameters exceeds a certain limiting value, we observe bifurcation of the dynamics which we discuss subsequently. Finally we focus on the features of chaotic behavior of the robot gait.

### 7.1 Symmetric gait

This section presents the evolution of pertinent gait descriptors as functions of the three parameters during the symmetric gait regime of the robot. As opposed to a parameters which can be directly altered, a gait descriptors is an observed(measurable or computable) quantity which cannot be modified directly but is indirectly influenced by the parameters. The gait descriptors that appear the most meaningful to us for this study are the state variables  $q$ , the half inter-leg angle at touchdown  $\alpha$ , the step period  $T$ , the average speed of progression  $v$ , the total mechanical energy of the robot  $E$ , and the loss of mechanical energy  $\Delta E$  due to impact.

The evolution of the gait descriptors is presented in the form of so-called bifurcation. Figs.5(a) to 5(f), 6.(a) to 6.(f) and 7(a) to 7(f). present the evolution of the gait descriptors that appear the most meaningful to us for this study are the state descriptors  $T$ ,  $\alpha$ ,  $\dot{\theta}_s$  (at the beginning of a step),  $v$ ,  $E$  and  $\frac{\Delta E}{E}$  as functions, respectively, of the parameters  $\phi$  and  $\mu$  but decreases with  $\beta$ . The results show that both the step period and the step length of the robot. The overall behavior of the robot can be summarized qualitatively as follows:

	T	L	E	v
$\phi \nearrow$	$\nearrow$	$\nearrow$	$\nearrow$	$\nearrow$
$\mu \nearrow$	$\nearrow$	$\nearrow$	$\nearrow$	$\nearrow$
$\beta \nearrow$	$\nearrow$	$\nearrow$	$\searrow$	$\searrow$

Some interpretations are in order here. Let us consider the evolution of total mechanical energy  $E$  of the robot in response to parameter changes. As the ground slope  $\phi$  increases the potential energy  $PE$  of the robot available per step slightly increases. The kinetic energy  $KE$ , being roughly proportional to  $\|\dot{\theta}\|^2$ , increases also, see Fig.5(c). As a consequence the total energy  $E$ , Fig.5(e). An increase in  $\beta$  results in a lowering of the center of mass of the robot, which lowers  $PE$  available per step and increases the step period. The latter results in a decreases in the average velocity of the robot (Fig.7 (d)). The increase in  $KE$  caused by the small increase in the  $\dot{\theta}_s$  cannot compensate for the decreases in  $PE$  and consequently lowers  $E$ . Conversely, an increase in  $\mu$ , which results in raising the center of mass of the robot, increase  $E$ .

It is interesting to look at the effect of a parameter change on the evolution of entire limit cycles as shown in Fig.s5(g), 6(g) and 7(g). In response to an increase in  $\phi$  the limit cycle expands along both axes, see Fig.5(g), implying an increase in the range of joint angle and joint velocity. The limit cycles are compensated along the joint velocity axis for an increase

in the parameters  $\mu$  and  $\beta$  (Figs .6(g) and 7(g)). A shorter reach of the limit cycle along the joint velocity axis means a smaller maximum joint velocity but dose not necessarily mean a slower robot . We see in Fig6 (d) that an increase in  $\mu$  is associated with an increase in the average speed of progression  $v$  .

## 7.2 Chaotic bifurcation

### 7.2.1 Period-doubling bifurcation

We noticed in Figs.5 and 6 that for the range of variations of the parameters considered in this study an increase in  $\phi$  and  $\beta$  cause a bifurcation in all the gait descriptors. Bifurcation was also observed for higher values of  $\mu$  especially when coupled with higher values of  $\phi$  (Fig.7).

As a consequence of the period-doubling bifurcation the limit cycle becomes 2-periodic and the robot gait becomes asymmetric with a shorter step and a longer step. The occurrence of bifurcation is shown in Figs.5,6,7 by the emergence of two branches in the curves, each associated with one of two dissimilar steps and describing its characteristic variables. Since bifurcation involves the state of the system and since all the gait descriptors, in turn, depend on the robot states, the occurrence of bifurcation is simultaneously manifested in all the gait descriptors.

On further increasing the parameters , the robot gait may experience a further period-doubling, giving rise to a 4-periodic limit cycle . This phenonmenon , repeated ad infinitum, is called a period doubling cascade and is recognized as one of the possible routes leading to chaos. Regardless of the parameter considered, we observe that the successive period doubling occur after progressively smaller intervals of parameter variation. This is expected in view of general results on period doubling casacades.

Period doubling cascades leading to chaotic behavior have already been observed for passive planar hopping robots which possess a smaller dimension than that of the compass.  $2^n$ -periodic gaits, termed as "limping gaits," were observed and analyzed for hopping robots.

In Fig.9 we introduce a novel way of capturing the behavior of the biped during a period doubling cascade ensuring from the parameter  $\phi$  (other parameters are kept constant at  $\mu = 2, \beta = 1$ ). The figure plots the first return map of  $\theta_{ns}$  . For a 1-periodic robot gait  $\theta_{ns}$  is the same in every step. This gait is therefore represented by a point on the  $45^\circ$  line.

As we change the ground slope, this point moves along the  $45^\circ$  line from the right-hand top corner of Fig.9, as indicated by the arrow.

The first period doubling occurs at  $\phi = 4.38^\circ$  when the gait turns 2-periodic and is therefore represented by 2 points. Just after the first bifurcation the 2 representative points differ only slightly from that of the 1-periodic gait from which they originate. The two steps are therefore very similar to the steps of the symmetric gaits. On further changes , in the parameter the two representative points move away from the  $45^\circ$  line along the two branches shown by dotted lines in Fig.9. It follows that one step length is slightly longer and the other slightly shorter than those of the corresponding symmetric gait. As we increase the slope the longer step is further elongated and the shorter step further shortened.

This continues until a second period doubling occurs at  $\phi = 4.93^\circ$  when each branch gives rise to two sub-branches. In this 4-periodic gait the 4 different steps are visited in the same

order with a longer step always followed by a shorter step. The last clearly identifiable bifurcation occurs when  $\phi = 5.02^\circ$  as the robot gait becomes 8-periodic.

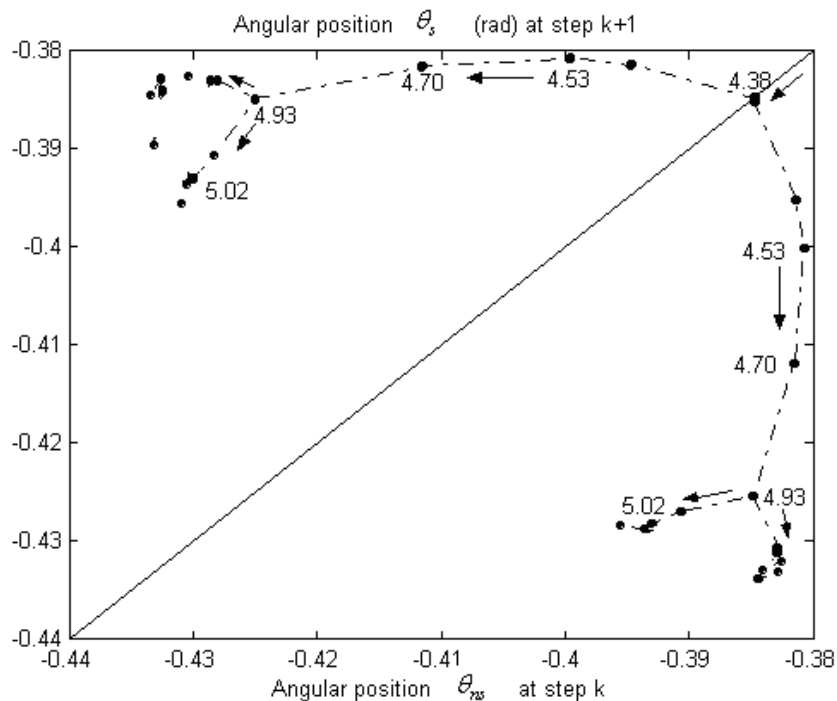


Fig. 20. First-return map of  $2^n$ -periodic steady gaits

The period doubling cascade may also be observed using phase plane diagrams. The phase plane diagram for a symmetric gait, which is a single-loop closed trajectory repeated after two robot steps. During one step the considered leg is in the swing stage and during the following one, it is in the support stage. Since the gait is symmetric, the robot legs are indistinguishable and the phase plane cycles of the two legs are identical.

In case of a 2-periodic gait, since all state variables are identical after every two steps, the phase plane limit cycle associated with one leg is still a single-loop closed trajectory repeated after two robot steps, see Fig.21(a). However, since the gait is asymmetric, the limit cycles associated with the legs are no longer identical.

In case of  $2^n$ -periodic gaits, all the state variables repeat themselves after every  $2^n$  steps. The phase plane diagram associated with one leg is therefore a  $2^{n-1}$ -loop closed trajectory repeated after every  $2^n$  steps, distinguishable from the phase diagram of the other leg. The visual inspection of the phase plane diagrams of the 4-periodic and the 8-periodic gaits (Fig. 21(b) and 21(c), respectively) correctly indicates that they resulted from the bifurcation of respectively the preceding 2-periodic and the 4-periodic gaits.

### 7.2.2 Chaotic gaits

The chaotic gait is an extreme case of the asymmetric gait and is characterized by a complete disappearance of order in a system. During a chaotic gait on a given slope, the states, and consequently the gait descriptors, of the biped robot never completely repeat themselves. Chaotic gaits are represented in the bifurcation diagrams by a continuous distribution of points. We explicitly show this on Figs.22(a) and 22(b) and omit them in the other bifurcation diagrams for the sake of clarity.

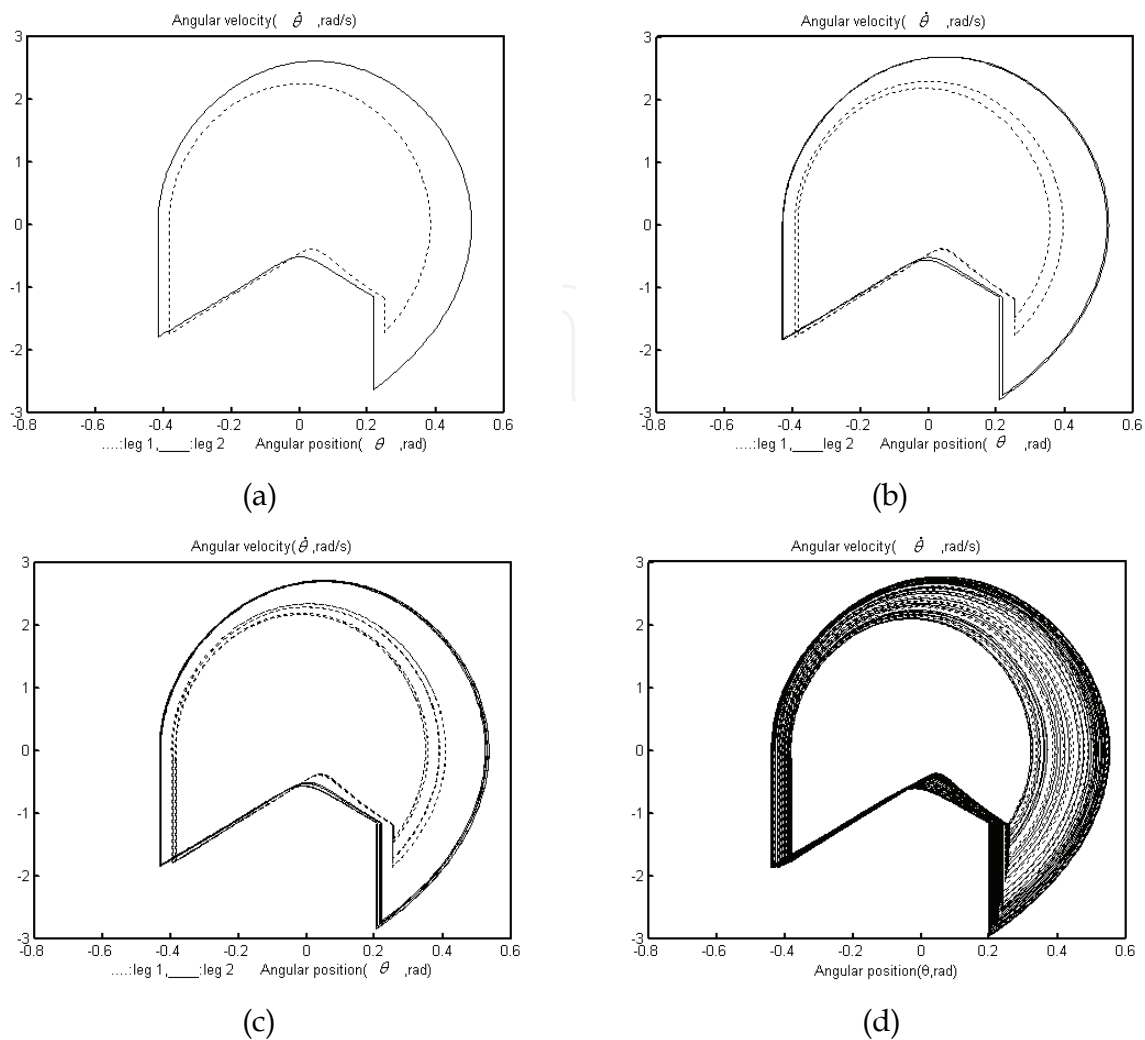


Fig. 21. Phase plane limit cycles of a) 2-periodic steady gait( $\phi = 4.38^\circ$ ), b) 4-periodic steady gait( $\phi = 4.93^\circ$ ), c) 8-periodic steady gait( $\phi = 5.02^\circ$ ) d) chaotic gait associated with one leg, 100 robot steps, ( $\phi = 5.2^\circ$ ). For all the 4 subplots  $\mu = 2, \beta = 1$ .

The gradual progression of the robot gait to the chaotic regime is well depicted in the first return maps of  $\theta_{ns,k+1} = f(\theta_{ns,k})$  shown in Figs. 11(a) to 11(d). When  $\phi = 5.02^\circ$ , the gait is 8-periodic and its first return map consist of 8 points. At  $\phi = 5.05^\circ$ , the first return map still consists of 8 distinguishable clusters of points(Fig.11(a)). Through multiple period doubling bifurcation this 8-periodic gait gives rise to a  $2^n$ -periodic gait with a large  $n$ . This gait will still preserved and  $\theta_{ns}$  is still always followed by a small one. The same property is still preserved, since a large  $\theta_{ns}$  is still always followed by a small one. The same property still holds for  $\phi = 5.13^\circ$ , but in this case the first return map appears as a continuum of points(Fig.11(c)). We are therefore very close to the "broad-band frequency" characteristic typical of chaotic behavior. Finally, when  $\phi = 5.21^\circ$ , we observe that predictability and periodicity have been completely destroyed, since a large  $\theta_{ns}$  can be followed by another large one. The layered structure of the strange attractor can also be guessed from the first return map.

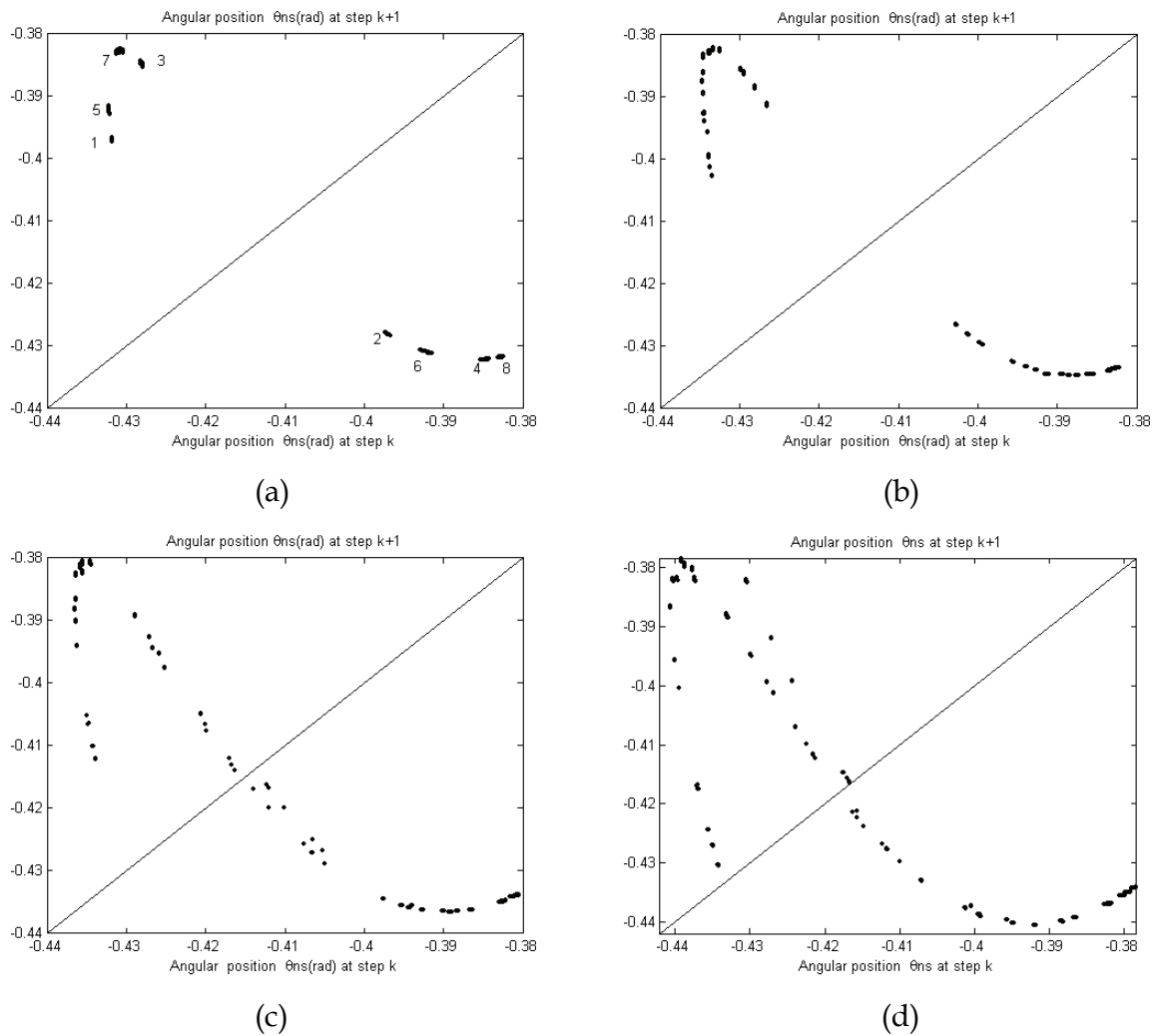


Fig. 22. First return map of  $\theta_{ns}$  : a)  $2^n$ -periodic gait,  $n$  large ( $\phi = 5.05^\circ$ ), b)  $2^n$ -periodic gait,  $n$  very large ( $\phi = 5.10^\circ$ ), c) approaching chaotic gait ( $\phi = 5.13^\circ$ ), d) chaotic gait ( $\phi = 5.21^\circ$ ). For all the 4 subplots  $\mu = 2, \beta = 1$ .

### 7.2.3 Local stability of the limit cycle

One way to investigate the orbital stability of a limit cycle is by means of studying the stability of its fixed point in the Poincare map. As a natural choice studying of the Poincare section of the compass biped we take the condition that the swing leg of the robot touches the ground. For two successive touchdowns of the same leg the states of the robot can be related as

$$x_k = F(x_{k+1}) \quad (14)$$

Where  $x = [\theta_{ns}, \theta_s, \dot{\theta}_{ns}, \dot{\theta}_s]^T$  is the 4-component state vector of the robot.

For a cyclic phase trajectory the first return map is fixed point of the mapping. On a cyclic trajectory, therefore,  $x_k = x_{k+1}$  and we can write,  $x^* = F(x^*)$ . For a small perturbation  $\Delta x^*$  around the limit cycle the nonlinear mapping function  $F$  can be expressed in terms of Taylor series expansion as

$$F(x^* + \Delta x^*) \approx F(x^*) + (\nabla F)\Delta x^* \tag{15}$$

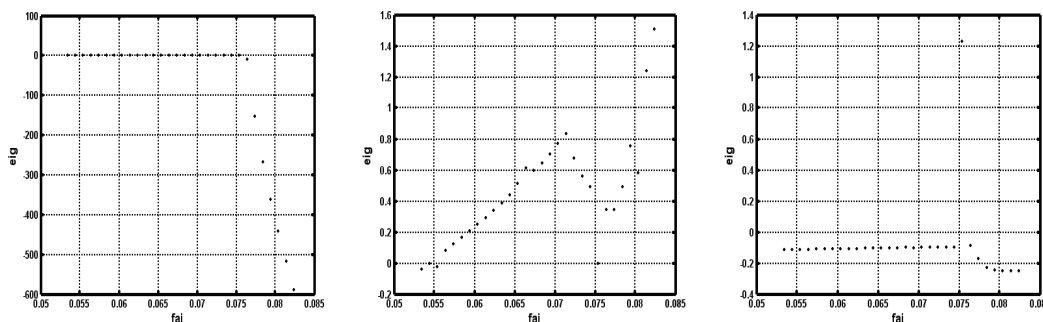
Where  $\nabla F$  is the gradient of  $F$  with respect to the states. Since  $x^*$  is a cyclic solution, we can rewrite Eq.2as

$$F(x^* + \Delta x^*) \approx x^* + (\nabla F)\Delta x^* \tag{16}$$

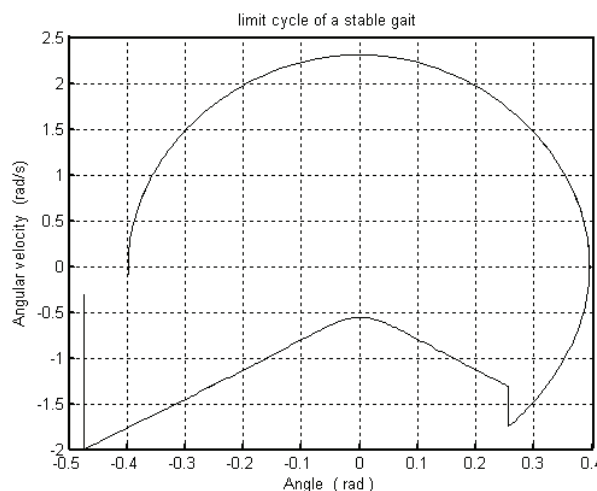
The mapping  $F$  is stable if the first return map of a perturbed state is closer to the fixed point. This property can be viewed as the contraction of the phase eigenvalues of  $\nabla F$  at the fixed point  $x^*$  are strictly less than one. From Eq.3 we write  $(\nabla F)\Delta x^* \approx F(x^* + \Delta x^*) - x^*$  where  $F(x^* + \Delta x^*)$  is the first return map of the perturb one state  $x^* + \Delta x^*$ . As it is not practical to analytically calculate perturb one state at a time by a small amount and observe its first return map. Repeating this procedure at least four times (once for each of the four states) we obtain an equation of the form

$$(\nabla F)\tau = \Psi \tag{17}$$

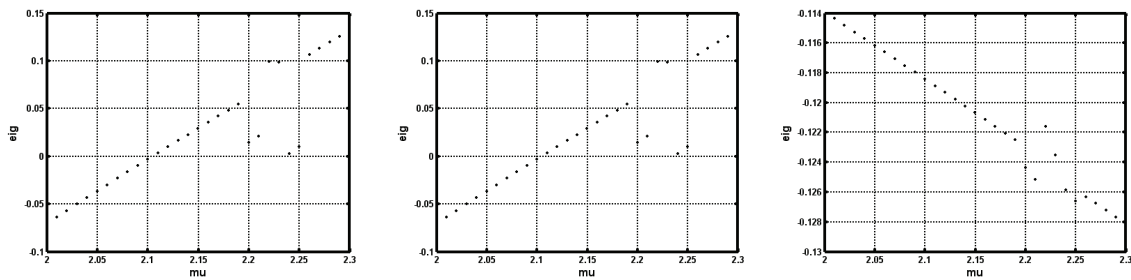
When  $\phi$  increases from 0.0524 to 0.0824, the variation of eigenvalues are as follows:



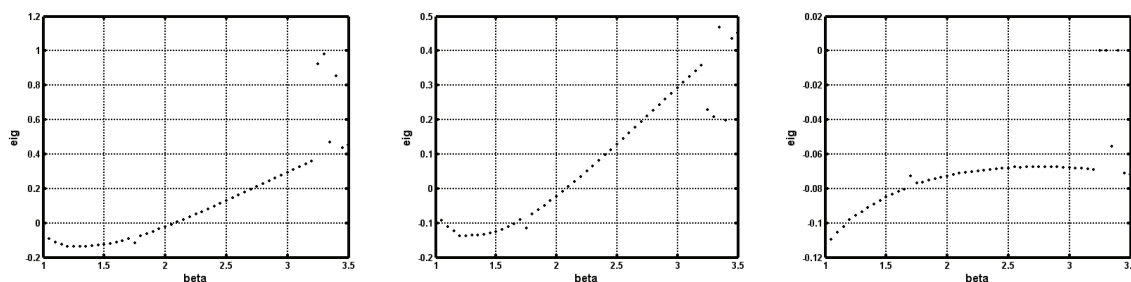
When  $\phi = 0.0908$ , the limit cycle is as follows:



When  $\mu$  increases, the variation of the first, the second and the fourth eigenvalues are as follows:



When  $\beta$  increases, the variation of the first, the second and the fourth eigenvalues are as follows:



When  $\mu$  and  $\beta$  increase, the real parts of the first and the second vary from negative to positive. It shows that the system varies from stable to unstable.

#### 7.2.4 Chaotic control laws

Here we introduce a simple control law which was inspired by the passive energy characteristics of the compass model. As the robot walks down on a slope its support point also shifts downward at every touchdown. As it loses gravitational potential energy in this way its kinetic energy increases accordingly. In a steady walk this is exactly the amount of kinetic energy that is to be absorbed at the end of each step by the impact. If, at every touchdown we reset our potential energy reference line to the point of touchdown, the total energy of the robot appears constant regardless of its downward descent. We formulate a control strategy for the robot based on this principle. The control law, aware of this characteristic energy of the passive limit cycle, called the *reference energy* in this section, of the robot on a given slope tries to drive the robot toward it.

### 8. The introduction of anti-phase synchronization

Observing from the human gait biped, symmetry is an important indicator of healthy gait[6]. The presence and nature of asymmetry in gait can be a useful diagnostic tool for the clinicians. Symmetry can be measured through the use of so many kinetics variables such as acceleration, force, moment, energy, power, step period and step length. Is it possible to apply this obviously symmetry property of healthy gait in human walking into the design of the robot's gait and explicitly explain the efficiency of human and animal locomotion more in detail will be a new challenge. Some new control strategy of "anti-phase synchronization" has been presented here to reduce the complexity such as the property of nonlinearity and strong coupling of this hybrid dynamic system. To the best of our knowledge, it is the first time to introduce the concept of synchronization to explain and control the motion of passive biped theoretically.

For a perfectly symmetric gait a properly synchronized twin trajectories from corresponding joints should be identical. Through the control and the reduced presumption of the collision model, the strong coupling between two legs has been successfully erased. A controller which is able to solve the synchronization problem in such a way that the pendulum reaches the desired level of energy and they move synchronously in opposite directions has been presented and in addition the construction of new Lyapunov function and simulation results prove the validity of the strategy. The method stated in the paper is helpful to practical application of the design of the robot's gait.

The paper is organized as follows. First we formulate the problem statement. Next we analyze the behavior of compass-like biped. Then the symmetry property in gait biped and the possibility to the application of the anti-phase synchronization have been discussed in III as well as the problem of erasing the coupling between two legs. The main contribution of V is the construction of Lyapunov function, the proposed controller and also the local stability analysis. Simulation results stated in IV just verify the effectiveness of the proposed method. The conclusions and future work are formulated in the final part.

### 8.1 Some symmetry property in gait biped

One of the most important properties in steady gait biped is that there exists some kind of symmetry with the variation of angle position and angle velocity.

The comparison relationship on the angular position of the two legs during steady periodic gait cycle has been presented in Fig. 3. It is obviously that angular positions of the two legs are asymmetry. The gait biped walking works as a double pendulum, while the stance leg has a comparative big difference with the swing leg. This can be explained that the stance leg experiences a relative compelled motion with the action force coming from the swing leg as well as from gravity. And in addition, the coupling degree of the two legs varies at different instant.

Presume the intersection point between two legs in Fig. 3 and the middle point with the two culmination value within one cycle of the swing leg as the symmetry point respectively, we get the asymmetry degree figures about two legs.

Observing from Fig. 4(a), different hip mass will correspond to the result that the larger the hip mass is, the higher the symmetry degree is. That is to say, the coupling effect between two legs will be influenced by the hip mass in great degree. With Fig. 4(b), different  $\mu$  will correspond to the different error about the angular position and angular velocity. The conclusion is very important for it will help in modifying the gait biped model when choosing the parameter and adjusting the gait biped cycle. As stated above, Figures 4(a) and 4(b) just provide us a kind of symmetry. While for the coupling of the two legs, it is impossible to construct the same ideal sub-systems to fulfil traditional master-slave synchronization corresponding to the dynamic system of the robot. The most direct way is to erase the coupling of the two legs and construct the subsystem of the swing leg and stance leg respectively, observing their position and the angle velocity relationship.

### 8.2 Anti-phase synchronization

In order to make the system to reach a kind of synchronization, the complex dynamic equation should be simplified as: 1. erase the coupling of two legs. 2. construct the new collision model between the swing leg and the ground. 3. add the control with the least energy consumption at appropriate instant as impulse force to imitate the behaviour of human gait. The paper will pay great attention to the solution of the first problem.

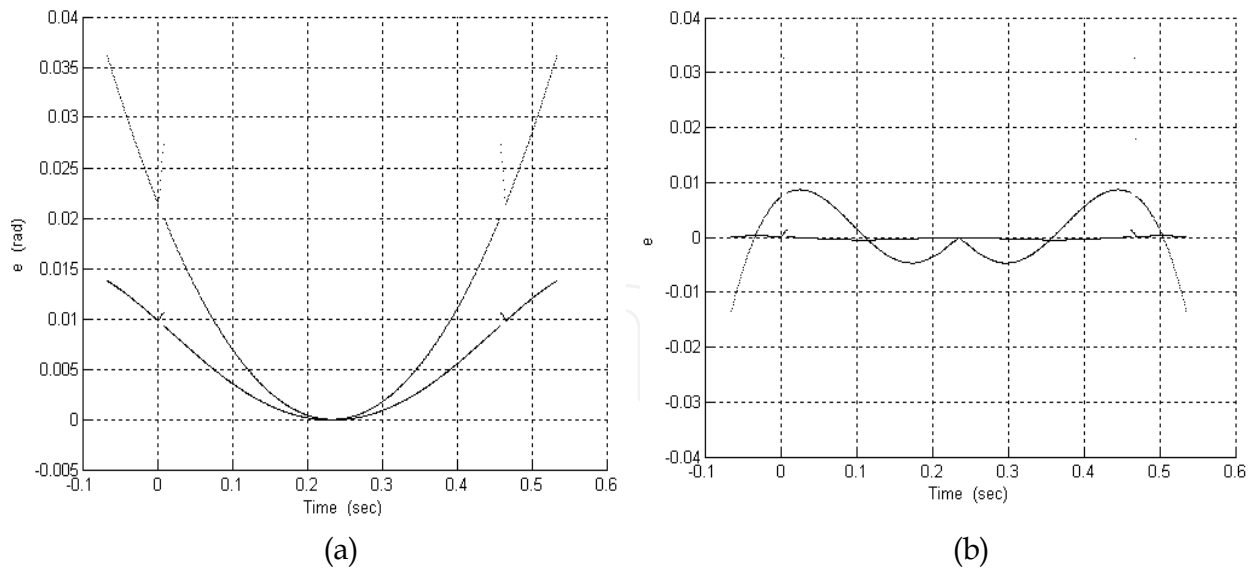


Fig. 23. The asymmetry degree Figures about two legs with different symmetry point (a) inter-section point between legs (b) centre value with two culmination within one cycle of the swing leg

By applying the idea of “inverse dynamic control” [10], make both the gravity torque act on the robot and the added control torque be equivalent to a gravity action, then a closed loop linear system with the same effect on the robot can be obtained. The advantage of the idea is that it can help adjust the gait distance and also the period corresponding to the forward varied velocity at any instant. Through the control, the swing leg acts as the single pendulum and the stance leg works as the inverted pendulum, the dynamic property of the two legs are the same except the analysis of the equilibrium point and the stability.

In addition, a reasonable presumption can be provided that there exists no collision with the swing leg and the ground with respect to this kind of pendulum walking. That means with the algebra constraint added, during the cycle of gait biped, the tip of the swing leg slides with the ground all the time and no friction will be considered when the robot moving forward. The construction of the new collision model can be solved by the consideration of knees which is not the topic of this paper. It is reasonable for us to eliminate the impact of collision model here for the impact can be solved by some idea such as time delay set and other counteract equipment when designing the real robot. Under this condition, the phase graph of the gait will be a perfect circle, at the end of each gait cycle, the velocity of the leg will be set zero and at the same time preceding the velocity conversion.

### 8.3 Erasing the coupling

There exists strong coupling action between  $\theta_{ns}$  and  $\theta_s$  when analysing the dynamic equation. Erasing the coupling and construct the same sub-system with the idea of “inverse dynamic control”, then obtain a closed loop linear system. For the non-linear equations (2) of our biped, as the stance leg is about to leave the ground, the anti-phase control is induced to the equation with the form

$$u = B^{-1}(M(\dot{q})a + C(q, \dot{q})\dot{q} + g(q)) \quad (18)$$

Reduces the system to the decoupled double integrator system

$$\ddot{q} = a \quad (19)$$

Joint angles can then be controlled independently using a control law

$$a = -K_p q - K_d \dot{q} + r \quad (20)$$

Where  $K_p$  and  $K_d$  are diagonal matrices with elements consisting of position and velocity gains, respectively. For a given desired trajectory

$$t(q^d(t), \dot{q}^d(t)) \quad (21)$$

We can choose the input  $r(t)$  as

$$r = \ddot{q}^d(t) + K_p q^d(t) + K_d \dot{q}^d(t) \quad (22)$$

The desired trajectory can be obtained as cubic trajectory as shown in [11] if the initial and final states of the trajectory are known. Thus a kind of synchronization can get with the walking trajectory and the given trajectory.

Simulation demonstrates that the rule for the swing leg is similar with the simple pendulum, during the process of anti-phase synchronization control, keep the dynamic state of the swing leg and make the stance leg act with the same rule, then

$$a = \begin{bmatrix} -\frac{g}{kl} \sin(\theta_{ns} + \phi) \\ -\frac{g}{kl} \sin(\theta_s + \phi) \end{bmatrix} \quad (23)$$

$k$  is the parameter representing the mass centre of the pendulum. With the same parameter described in section 2, the distance between the hip and the mass centre is  $b$ , the distance between the foot and the mass centre is  $a$ , where  $k = \frac{\beta}{\beta + 1}$ ,  $\beta = \frac{b}{a}$ .

The dynamic equation of the robot can be divided into two independent parts, and both of them possess the same expression as

$$\ddot{\theta}_{ns} + \frac{g}{kl} \sin(\theta_{ns} + \phi) = 0 \quad (24)$$

$$\ddot{\theta}_s + \frac{g}{kl} \sin(\theta_s + \phi) = 0 \quad (25)$$

#### 8.4 Control synchronization

For global application of the synchronization method, introduce the new coordination

$$\theta_{ns}^t = \theta_{ns} + \phi$$

$$\theta_s^t = \theta_s + \phi$$

With the control strategy stated above, equations of the two legs have been given as (9) and (10) with the same dynamic control rule. Assume that both the legs possess the point mass  $m$ , and then the virtual mechanical energy of the robot is

$$V = \frac{1}{2}m(kl)^2(\theta_{ns}^t + \theta_s^t) + mgkl(1 - \cos\theta_{ns}^t) + mgkl(1 - \cos\theta_s^t) \quad (26)$$

Obviously  $V \geq 0$ , appoint  $V$  as the Lyapunov function of the system, for the collision has been avoided here, thus the system is conservative, then  $\dot{V} = 0$ . Seen from equation (11), the mechanical energy of the system is constant, this proves that the dynamic behaviour of the two legs can come to the state of anti-phase synchronization; expected ideal symmetry property appears here.

Synchronizing the two dynamic systems with the idea (12) so called mutual direction coupling synchronization.

$$\begin{cases} \dot{\bar{x}} = f(\bar{x}) + \bar{K}(\bar{x} - \bar{x}) \\ \dot{\bar{x}} = f(\bar{x}) + \bar{K}(\bar{x} - \bar{x}) \end{cases} \quad (27)$$

Where  $\bar{K}(\bar{x} - \bar{x})$ ,  $\bar{K}(\bar{x} - \bar{x})$  is the mutual coupling synchronization control item of the two sub-systems. In addition, it will be adjusted different for the purpose of improving the synchronized precision and enhancing the synchronized velocity.

$K = \text{diag}(k_1, k_2, \dots, k_n)$  is so called coupling length, where  $n = 2$  here. Therefore the control objective can be formalized by the following relations

$$\lim_{t \rightarrow \infty} (\theta_{ns}^t + \theta_s^t) = 0 \quad (28)$$

$$\lim_{t \rightarrow \infty} (\dot{\theta}_{ns}^t + \dot{\theta}_s^t) = 0 \quad (29)$$

Synchronized time of the system should be considered here and two legs would come to the state of anti-phase synchronization within one cycle with the control. In order to fulfil the control of the gait biped, two main problems are discussed as follows: 1. stability with which the robot will not to slip forwards or downwards corresponding to the gait biped in a 2-dimension plain. 2. the gait should satisfy any given target velocity and gait distance as well. To reach this kind of target control goal, an applicable method is to control the amplitude of the swing leg with energy consumption consideration.

Add the new controller which is related to in system (9) and (10)

$$\ddot{q} = a + \bar{B}u \quad (30)$$

Where

$$\bar{B} = \begin{bmatrix} 1 & 0 \\ -1 & 1 \end{bmatrix}$$

$$u = \begin{bmatrix} -\gamma \dot{\theta}_{ns}^t H - \lambda_1 \sin(\theta_{ns}^t + \theta_s^t) - \lambda_2 (\dot{\theta}_{ns}^t + \dot{\theta}_s^t) \\ -2\gamma \dot{\theta}_{ns}^t H - 2\lambda_1 \sin(\theta_{ns}^t + \theta_s^t) - 2\lambda_2 (\dot{\theta}_{ns}^t + \dot{\theta}_s^t) \end{bmatrix} \quad (16)$$

Where  $H = H(\theta_{ns}, \dot{\theta}_{ns}) + H(\theta_s, \dot{\theta}_s) - 2H^*$ .  $\lambda_1, \lambda_2$  is the ratio coefficient, which decides the converging speed of anti-phase synchronization;  $\gamma$  is positive gain coefficient.  $H$  represents Hamiltonian function of each pendulum-like leg and the designed controller (16) can swing the pendulum up to the desired energy level  $H^*$  in such a way that the pendulum-like two legs move in opposite directions.

**Theorem:** For any given controller presented as (16), if satisfies  $\lambda_2 > 2H^*$ , then the set  $\theta_{ns}^t = -\theta_s^t, \dot{\theta}_{ns}^t = -\dot{\theta}_s^t$  is globally asymptotically stable with respect to the controlled system (15).

**Proof:** Construct the virtual Hamiltonian function of each pendulum-like leg

$$H(\dot{\theta}, \ddot{\theta}) = \frac{1}{2} m(kl)^2 \dot{\theta}^2 + mgkl(1 - \cos \theta^t) \quad (31)$$

The control objective can be formalized by the following relations

$$\lim_{t \rightarrow \infty} H(\theta(t), \dot{\theta}(t)) = H^* \quad \theta = \theta_{ns}^t, \theta_s^t \quad (32)$$

The relation implies that the periods of oscillations of each pendulum are identical (frequency synchronization).

Using the control law (16), analyses the equations of the closed loop system with respect to the variable  $x = \theta_{ns}^t + \theta_s^t$ , then

$$\begin{aligned} & m(kl)^2 \ddot{x} + \lambda_2 \dot{x} + \lambda_1 \sin x \\ & = -\gamma [H(\theta_{ns}^t, \dot{\theta}_{ns}^t) + H(\theta_s^t, \dot{\theta}_s^t) + \lambda_2 - 2H^*] \dot{x} \end{aligned} \quad (33)$$

Define a new Lyapunov function to the whole system

$$\begin{aligned} V &= \frac{1}{2} m(kl)^2 \dot{x}^2 + \lambda_2 (1 - \cos x) \\ &+ mgkl(2 - \cos \theta_{ns}^t - \cos \theta_s^t) \end{aligned}$$

Obviously  $V \geq 0$

$$\begin{aligned} \dot{V} &= m(kl)^2 \dot{x} \ddot{x} + \lambda_2 \dot{x} \sin x \\ &= -\gamma [H(\theta_{ns}^t, \dot{\theta}_{ns}^t) + H(\theta_s^t, \dot{\theta}_s^t) + \lambda_2 - 2H^*] \dot{x}^2 \end{aligned}$$

for  $H(\theta_{ns}^t, \dot{\theta}_{ns}^t) \geq 0, H(\theta_s^t, \dot{\theta}_s^t) \geq 0$ , if  $\lambda_2 > 2H^*$ ,  $\dot{V} \leq 0$ . Then the set  $x=0$  is globally asymptotically stable.

From this observation one can make a few important conclusions. First, the uncontrolled system can exhibit synchronous behaviour. Clearly, it follows that the Hamiltonian of each

pendulum tends to a common limit. However, due to energy dissipation the limit value depends on the initial conditions and particularly, if one initializes the pendulum from an identical point, the oscillations will decay. Therefore the uncontrolled system exhibits a behaviour which is very close to the desired one, and there is one thing to the controller-to maintain the energy level for each pendulum, and this problem will be useful for the further research.

As predicted by the theorem, there is a set of zero Lebesgue measure of exceptional initial conditions for which the control objective can not be achieved. For example, if one initiate the system at the point where  $\theta_{ns}^t = \theta_s^t = 0$ ,  $\dot{\theta}_{ns}^t = \dot{\theta}_s^t = 0$  the anti-phase synchronization control  $\bar{u}$  based on the energy can't drive the system away from the zero condition, however from practical point of view, it is not difficult to modify the controller to handle this problem.

Presume the system has been in the condition of anti-phase synchronization, that is, the stable point of the closed loop system, the limit dynamics of each pendulum is given by the following equation

$$m(kl)^2 \ddot{\theta}^t + mgkl \sin(\theta^t) = -2\gamma [H(\theta^t, \dot{\theta}^t) - H^*]$$

And therefore the control objective

$$\lim_{t \rightarrow \infty} H(\theta^t, \dot{\theta}^t) = H^*$$

is achieved.

### 8.5 Simulation and discussion

To verify the effectiveness of the proposed method, we conduct the following simulation results.

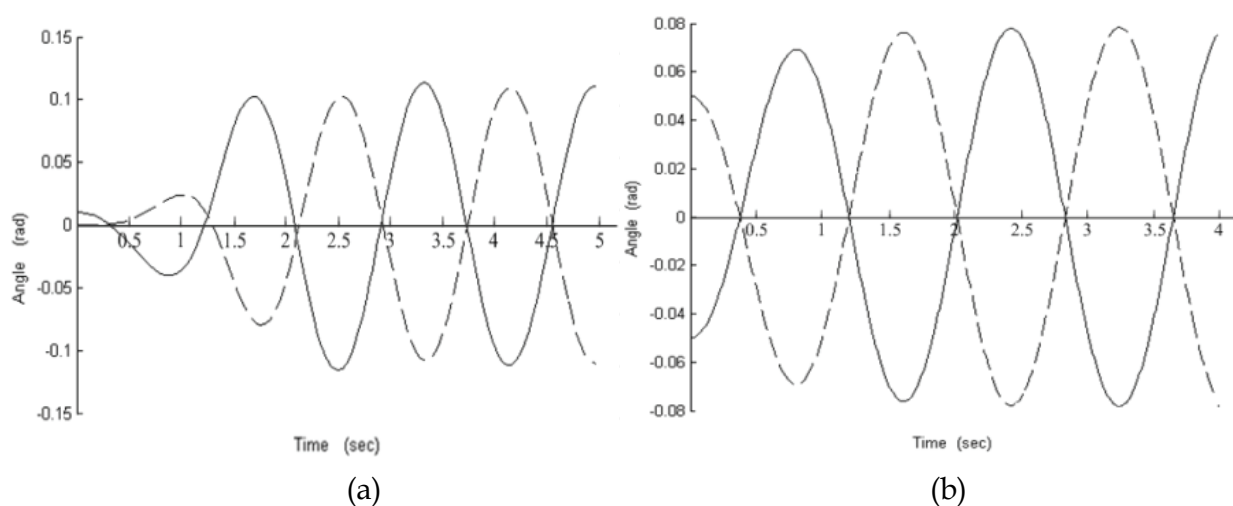


Fig. 24. Anti-phase synchronization of two legs in the controlled system with different initial condition  $(\theta_{ns}, \theta_s, \gamma)$  (a) (0.01, 0, 10) (b) (-0.05, 0.05, 10)

The limit cycle under anti-phase synchronization is given by Figure 5 and its Mechanical energy of the robot under anti-phase synchronization is just depicted by Figure 24. It is

clearly that the anti-phase synchronization can enlarge the convergence region of the limit cycle and it appears the typical double-pendulum property.

Figures 24 present the results of the anti-phase synchronization based on the energy control. With the anti-phase synchronization control, the angular position and angular velocity of the two legs can reach the synchronization with the same magnitude and the opposite direction at any moment. Simulation results prove the validity of the control method. In addition, as simulation demonstrates, with different initial condition of the gait biped will be around zero as well as any given biped value and with the control it can converge to the state of anti-phase synchronization corresponding to any given target energy. The converging speed depends on the controlled parameter  $\gamma, \lambda_1, \lambda_2$ . Virtually the higher the value of the parameters are, the faster the converging speed is. The consequence is valid with the consideration of both the constraint of the manipulator and the appropriate maximized sustaining force added on the system. In practice, for not using the initial condition as it does in simulation, so the effect of the control will be better in controlling the practical robot.

In this work, we considered the problem of controlled synchronization of the decoupled two legs based on the compass-like biped model. Some new method so called "anti-phase synchronization" has been presented to explain the perfectly symmetric gait typical of healthy gait in human walking. The paper also proposed a useful controller which is able to solve the synchronization problem in such a way that the pendulum reaches the desired level of energy and they move synchronously in opposite directions. In addition, the construction of Lyapunov function, the local stability analysis to the proposed controller as well as the presentation of simulation results have also been stated and proved the validity of the method.

For the next step, the design of a more efficient new collision model and also the further analysis about the added simplified impulse force under new condition will be helpful to practical application of the design of the robot's gait.

## 9. The description and assumption on he model with knees

Next, we will extend the model to the new one with knees, and the state of the straight direction of the gait biped will be equivalent to the one of the compass-like gait biped, then the equation can be united as the unanimous form discussed formerly the model shown as Figure 25, partially resemble Compass-like waker with point masse  $m_H$ ,  $m_s$  and  $m_t$  concentrated at the hip, shanks and thighs respectively. The leg-length is  $L$ , which is divided into three parts:  $l_s$  and  $l_t$ ,  $l_s$  is the distance from the heel to the knee of  $m$  and  $l_s$  is the distance from knee to the hip center  $m_H$ , in the meanwhile, both shank and thigh are divided by their respective sub-mass center  $m_s$  and  $m_t$  into two parts, with  $l_s$   $a_1$  and  $b_1$ , with  $l_t$   $a_2$  and  $b_2$ .  $l_s + l_t = L$ ,  $a_1 + b_1 = l_s$ ,  $a_2 + b_2 = l_t$ . As is depicted in figure 1, three key parameters are needed to describe the configuration of the walker,  $q_1$ ,  $q_2$  and  $q_3$ .  $2\alpha$  is the total angle between the legs, which is defined as the "inter-leg angle", and in addition is formed during the instant when both legs are touching the ground. The slope of the ground with the horizontal is denoted by the angle  $\gamma$ .

The model has been made by the following assumptions: the total mass of the robot  $m_C = 2m_s + 2m_t + m_H$  is constant. For the sake of analysing the model, we separate the

motion into two phases, knee-free phase and knee-locked phases, whose boundaries are knee-strike and heel strike, that is the period between knee-strike and heel-strike is knee-locked stage and the period between heel-strike and knee-strike is knee-free stage.

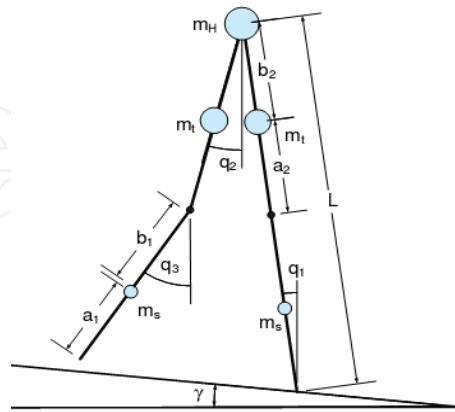


Fig. 25. Model of a passive kneed-walker on a slope

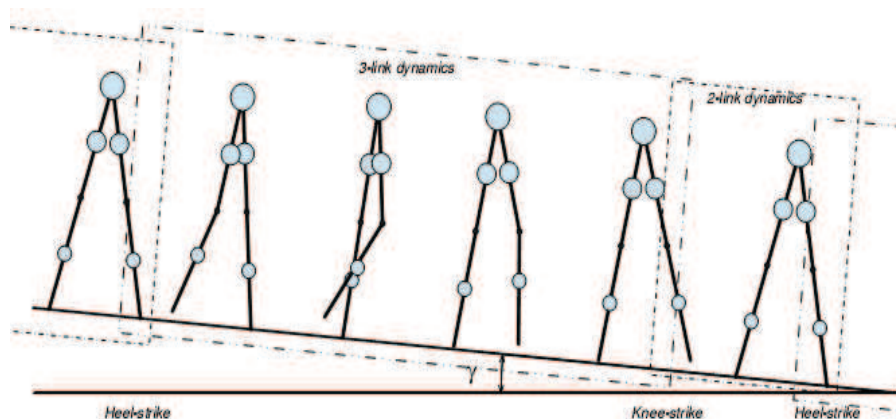


Fig. 2. Stages in a step cycle of a kneed-walker

In order to simplify the analysis and calculation of The waking model, we should make some assumptions at first. All masses are considered point-masses and one leg are identical with the other. The gait consists of knee-free stage and a knee-locked stage: during the knee-locked stage the robot behaves exactly like an inverted planar double pendulum with its support point being analogous to the point of suspension of the pendulum. During the knee-free stage, the stance leg remain straight while the swing-leg bends at its knee, which is different from the Compass-like walker. The robot is assumed to move on a horizontal or inclined plane surface. The impact of the swing leg with the ground is assumed to be inelastic and without sliding, so is the impact between the thigh and the shank of the swing leg, which marks the inception of the knee-locked stage. This implies that during the instantaneous transition stage the robot configuration remains un-changed, and the angular momentum of the robot about the impacting foot as well as the angular momentum of the pre-impact support leg about the hip are conserved. Thanks to angular-momentum conservation law, we can obtain some useful equations, by which some meaningful simulations will be made.

## 10. The applicable function on 3D model

As we have discussed before, we have finished the model of the whole integral process of the gait biped, while for the sake of the real application, a 3D model- a more anthropomorphic model should be presented necessarily.

The simulation of the 3D one is similar with the 2D model. Previously, when the roll angle and its derivative are set to zero, the equation gained from the support leg angle, non-support angle and their derivatives will be share some characteristics with the 2D robot. Moreover, reversely if the two angles and their derivatives are set to zero, the model represented by the roll angle will behave like an inverted pendulum. So the comparison between 3D model in this special condition and the 2D model is a direct way to the correct of the modeling.

### The 3d dynamic walking bipedal model

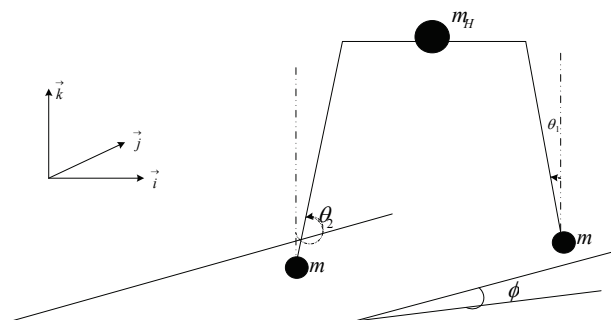


Fig. 26. 3d dynamical bipedal walker

The model consists of two legs connected by a pelvis, with pin joints at the hips[3]. The legs are point feet, shown as Figure.1. The same with 2D bipedal model, it is also equivalent to a double pendulum (more obviously in saggital plane model) with point masse  $m_H$  and  $m$  concentrated at the hip and feet respectively. The leg-length is  $l$ . The support angle  $\theta_1$ , nonsupport angle  $\theta_2$  and roll angle  $\theta_3$  determine the configuration of the gait. The angle was made by the biped leg with the vertical (counterclockwise positive).  $2\alpha$  is the total angle between the legs, which is defined as the "inter-leg angle", and in addition is formed during the instant when both legs are touching the ground. The slope of the ground with the horizontal is denoted by the angle  $\phi$ .

The model has been made by the following assumptions: the total mass of the robot  $m_C = 2m + m_H$  is constant and equal to 20kg. For the sake of simplifying the model, all masses are considered point-masses and the legs are identical with point feet. The same as 2d bipedal model, the 3d gait also consists of swing stage and an instantaneous transition stage: during the swing stage the robot behaves exactly like an inverted planar double pendulum with its support point being analogous to the point of suspension of the pendulum. During the transition stage the support is transferred from one leg to the other. The robot is assumed to move on an inclined plane surface and the leg only swing forward and backward. The impact of the swing leg with the ground is assumed to be inelastic and without sliding [4]. This implies that during the instantaneous transition stage the robot configuration remains un-changed, and the angular momentum of the robot about the

impacting foot as well as the angular momentum of the pre-impact support leg about the hip is conserved. These conservation laws lead to a discontinuous change in robot velocity.

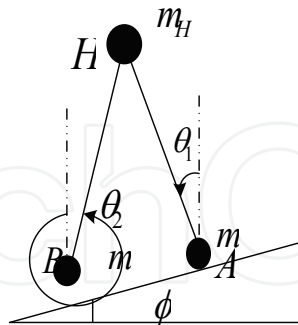


Fig. 27. Sagittal planar 3d model

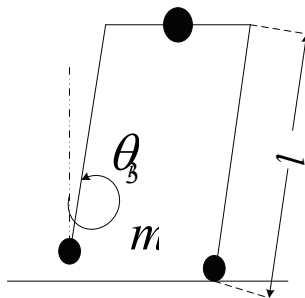


Fig. 3. Frontal 3d model

The new dynamic equations of the swing stage are similar to the well-known double pendulum equations. Since the legs of the robot are assumed identical, the equations are similar regardless of the support leg considered with the variation of the following.

$$M(\theta) = \begin{pmatrix} (m_H + m)L^2 & -mL^2 \cos(\theta_1 - \theta_2) & 0 \\ -mL^2 \cos(\theta_1 - \theta_2) & mL^2 & 0 \\ 0 & 0 & m_H L^2 \cos^2 \theta_1 + mL^2 (\cos \theta_1 - \cos \theta_2)^2 \end{pmatrix}$$

$$N(\theta, \dot{\theta}) = \begin{pmatrix} 0 & -mL^2 \dot{\theta}_2 \sin(\theta_1 - \theta_2) \\ mL^2 \dot{\theta}_1 \sin(\theta_1 - \theta_2) & 0 \\ L^2 \dot{\theta}_1 [-(m_H + m) \sin 2\theta_1 + 2m \cos \theta_2 \sin \theta_1] & 2mL^2 \dot{\theta}_2 (-\cos \theta_1 \sin \theta_2 + \sin \theta_2 \cos \theta_2) \\ mL^2 \dot{\theta}_3 \sin \theta_1 (\cos \theta_1 - \cos \theta_2) - m_H L^2 \dot{\theta}_3 \cos \theta_1 \sin \theta_1 \\ -mL^2 \dot{\theta}_3 \sin \theta_2 (\cos \theta_1 - \cos \theta_2) \\ 0 \end{pmatrix}$$

$$g(\theta) = \begin{pmatrix} -m_H g L \sin \theta_1 \cos \theta_3 - m g L \sin \theta_1 \cos \theta_3 \\ m g L \sin \theta_2 \cos \theta_3 \\ -m_H g L \cos \theta_1 \sin \theta_3 - m g L \cos \theta_1 \sin \theta_3 + m g L \cos \theta_1 \sin \theta_3 \end{pmatrix}$$

The parameters used for our simulations are  $l=1\text{ m}$ ,  $m_H=2\text{ m}=10\text{ kg}$ . Since no dissipation takes place during swing stage, thus the total mechanical energy  $E$  of the robot is conserved during this stage.

$$\frac{d}{dt} \frac{\partial L(\theta, \dot{\theta})}{\partial \dot{\theta}} - \frac{\partial L(\theta, \dot{\theta})}{\partial \theta} = 0$$

Where the Lagrangian  $L(\theta, \dot{\theta})$  is the difference between the kinetic energy and the potential energy of the robot:  $L(\theta, \dot{\theta})=K(\theta, \dot{\theta})-P(\theta)$ , the right-hand side term of (3) is 0, since the robot is completely passive. The new equation of the gait biped are given as the following and the results presented before can be applied perfectly.

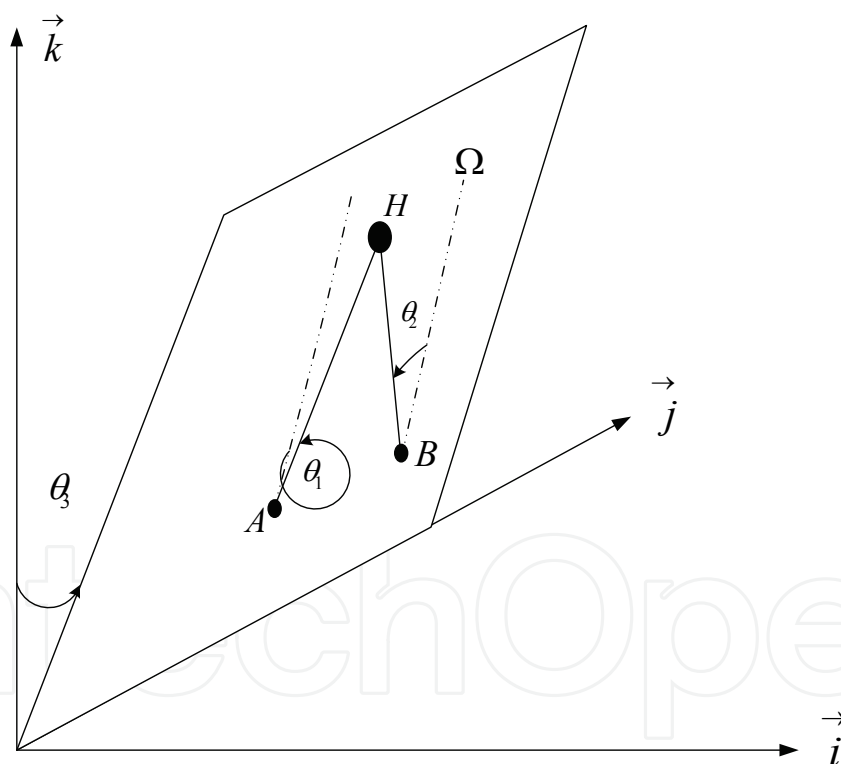


Fig. 19. Model in the 3d space

In order to calculate the energy of the robot, we simply consider the dynamics of the three distinct masses:

$$K(\theta, \dot{\theta}) = \frac{1}{2} m_H \left\| \vec{V}_H \right\|^2 + \frac{1}{2} m \left\| \vec{V}_B \right\|^2 + \frac{1}{2} m \left\| \vec{V}_A \right\|^2 \quad (34)$$

$$P(\theta) = m_H g L \cos \theta_1 \cos \theta_3 + m g L (\cos \theta_1 \cos \theta_3 - \cos \theta_2 \cos \theta_3) + P_0 \quad (35)$$

Where  $\vec{V}_H$ ,  $\vec{V}_A$  and  $\vec{V}_B$  are the velocities of the point masses. In the frame  $[\vec{i}, \vec{j}, \vec{k}]$  depicted on Fig.3, these vectors are given by:

$$\vec{V}_H = (-L\dot{\theta}_1 \sin \theta_1 \sin \theta_3 + L\dot{\theta}_3 \cos \theta_1 \cos \theta_3)\vec{i} + L\dot{\theta}_1 \cos \theta_1 \vec{j} + (-L\dot{\theta}_1 \sin \theta_1 \cos \theta_3 - L\dot{\theta}_3 \cos \theta_1 \sin \theta_3)\vec{k}$$

$$\begin{aligned} \vec{V}_B = & (-L\dot{\theta}_1 \sin \theta_1 \sin \theta_3 + L\dot{\theta}_3 \cos \theta_1 \cos \theta_3 + L\dot{\theta}_2 \sin \theta_2 \sin \theta_3 - L\dot{\theta}_3 \cos \theta_2 \cos \theta_3)\vec{i} \\ & + (L\dot{\theta}_1 \cos \theta_1 - L\dot{\theta}_2 \cos \theta_2)\vec{j} + (-L\dot{\theta}_1 \sin \theta_1 \cos \theta_3 - L\dot{\theta}_3 \cos \theta_1 \sin \theta_3 \\ & + L\dot{\theta}_2 \sin \theta_2 \cos \theta_3 + L\dot{\theta}_3 \cos \theta_2 \sin \theta_3)\vec{k} \end{aligned}$$

$$\vec{V}_A = 0$$

### The Transition equation

Since our robot is constituted of only two links, the condition of conservation of angular momentum leads to only two equations:

$$m_H \vec{V}_{H^-} \times \vec{A^-H^-} + m \vec{V}_{B^-} \times \vec{A^-B^-} = m_H \vec{V}_{H^+} \times \vec{A^+H^+} + m \vec{V}_{B^+} \times \vec{A^+B^+} \quad (36)$$

$$m \vec{V}_{A^-} \times \vec{H^-A^-} + m \vec{V}_{B^-} \times \vec{H^-B^-} = m \vec{V}_{A^+} \times \vec{H^+A^+} + m \vec{V}_{B^+} \times \vec{H^+B^+} \quad (37)$$

Where points H, A and B are respectively the hip, the mass center of the support leg, the mass center of the non-support leg.  $\vec{V}_H$ ,  $\vec{V}_A$  and  $\vec{V}_B$  are respectively the velocity vectors at H, A and B. The superscripts - and + indicate respectively pre-impact and post-impact variables. All the vectors appearing are given by:

$$\begin{aligned} \vec{V}_{H^-} = & (L\dot{\theta}_1 \sin \theta_1 \sin \theta_3 - L\dot{\theta}_3 \cos \theta_1 \cos \theta_3)\vec{i} + (-L\dot{\theta}_1 \cos \theta_1)\vec{j} + (-L\dot{\theta}_1 \sin \theta_1 \cos \theta_3 \\ & - L\dot{\theta}_3 \cos \theta_1 \sin \theta_3)\vec{k} \end{aligned}$$

$$\begin{aligned} \vec{V}_{A^-} = & (L\dot{\theta}_1 \sin \theta_1 \sin \theta_3 - L\dot{\theta}_3 \cos \theta_1 \cos \theta_3 - L\dot{\theta}_2 \sin \theta_2 \sin \theta_3 + L\dot{\theta}_3 \cos \theta_2 \cos \theta_3)\vec{i} + \\ & (-L\dot{\theta}_1 \cos \theta_1 + L\dot{\theta}_2 \cos \theta_2)\vec{j} + (-L\dot{\theta}_1 \sin \theta_1 \cos \theta_3 - L\dot{\theta}_3 \cos \theta_1 \sin \theta_3 \\ & + L\dot{\theta}_2 \sin \theta_2 \cos \theta_3 + L\dot{\theta}_3 \cos \theta_2 \sin \theta_3)\vec{k} \end{aligned} \quad \vec{V}_{B^-} = 0$$

$$\begin{aligned}\overrightarrow{V_{H^+}} &= (L\dot{\theta}_1 \sin\theta_1^+ \sin\theta_3^+ - L\dot{\theta}_3 \cos\theta_1^+ \cos\theta_3^+) \vec{i} + L\dot{\theta}_1 \cos\theta_1^+ \vec{j} \\ &+ (-L\dot{\theta}_1 \sin\theta_1^+ \cos\theta_3^+ - L\dot{\theta}_3 \cos\theta_1^+ \sin\theta_3^+) \vec{k}\end{aligned}$$

$$\begin{aligned}\overrightarrow{V_{B^+}} &= (L\dot{\theta}_1 \sin\theta_1^+ \sin\theta_3^+ - L\dot{\theta}_3 \cos\theta_1^+ \cos\theta_3^+ - L\dot{\theta}_2 \sin\theta_2^+ \sin\theta_3^+ + L\dot{\theta}_3 \cos\theta_2^+ \cos\theta_3^+) \vec{i} \\ &+ (L\dot{\theta}_1 \cos\theta_1^+ - L\dot{\theta}_2 \cos\theta_2^+) \vec{j} + (-L\dot{\theta}_1 \sin\theta_1^+ \cos\theta_3^+ - L\dot{\theta}_3 \cos\theta_1^+ \sin\theta_3^+ + L\dot{\theta}_2 \sin\theta_2^+ \cos\theta_3^+ + L\dot{\theta}_3 \cos\theta_2^+ \sin\theta_3^+) \vec{k}\end{aligned} \quad \overrightarrow{V_{A^+}} = 0$$

$$\overrightarrow{A^-H^-} = -L \cos\theta_2^- \sin\theta_3^- \vec{i} - L \sin\theta_2^- \vec{j} + L \cos\theta_2^- \cos\theta_3^- \vec{k}$$

$$\overrightarrow{H^-A^-} = L \cos\theta_2^- \sin\theta_3^- \vec{i} + L \sin\theta_2^- \vec{j} - L \cos\theta_2^- \cos\theta_3^- \vec{k}$$

$$\overrightarrow{A^+H^+} = -L \cos\theta_1^+ \sin\theta_3^+ \vec{i} + L \sin\theta_1^+ \vec{j} + L \cos\theta_1^+ \cos\theta_3^+ \vec{k}$$

$$\overrightarrow{H^+B^+} = L \cos\theta_2^+ \sin\theta_3^+ \vec{i} - L \sin\theta_2^+ \vec{j} - L \cos\theta_2^+ \cos\theta_3^+ \vec{k}$$

$$\begin{aligned}\overrightarrow{A^+B^+} &= (L \cos\theta_1^+ \sin\theta_3^+ + L \cos\theta_2^+ \sin\theta_3^+) \vec{i} + (L \sin\theta_1^+ - L \sin\theta_2^+) \vec{j} \\ &+ (L \cos\theta_1^+ \cos\theta_3^+ - L \cos\theta_2^+ \cos\theta_3^+) \vec{k}\end{aligned}$$

$$\begin{aligned}m_H[-\dot{\theta}_3 \cos\theta_1^- \sin\theta_2^- \sin\theta_3^- - \dot{\theta}_1 \cos\theta_3^- \cos(\theta_1^- - \theta_2^-)] &= m_H(\dot{\theta}_1 \cos\theta_3^+ + \dot{\theta}_3 \cos\theta_1^+ \sin\theta_1^+ \sin\theta_3^+) \\ &+ m[\cos\theta_3^+(\dot{\theta}_1^+ + \dot{\theta}_2^+) + (\dot{\theta}_1 - \dot{\theta}_2) \cos\theta_3^+ \cos(\theta_1^+ - \theta_2^+) - \dot{\theta}_3 \sin\theta_3^+ \sin(\theta_1^+ + \theta_2^+) \\ &+ \dot{\theta}_3 \sin\theta_3^+ (\cos\theta_1^+ \sin\theta_1^+ + \cos\theta_2^+ \sin\theta_2^+)]\end{aligned}$$

$$-m_H \dot{\theta}_3 \cos\theta_1^- \cos\theta_2^- = -m_H \dot{\theta}_3 \cos^2\theta_1^+ - m \dot{\theta}_3 (\cos\theta_1^+ - \cos\theta_2^+)^2$$

$$\begin{aligned}\dot{\theta}_1 \cos\theta_3^- \cos(\theta_1^- - \theta_2^-) - \dot{\theta}_2 \cos\theta_3^- + \dot{\theta}_3 \sin\theta_3^- \sin\theta_2^- (\cos\theta_1^- - \cos\theta_2^-) &= \dots \\ -\dot{\theta}_1 \cos\theta_3^+ \cos(\theta_1^+ - \theta_2^+) + \dot{\theta}_2 \cos\theta_3^+ + \dot{\theta}_3 \sin\theta_3^+ \sin\theta_2^+ (\cos\theta_2^+ - \cos\theta_1^+) &\end{aligned}$$

$$\dot{\theta}_3 \cos\theta_1^- \cos\theta_2^- - \dot{\theta}_3 \cos^2\theta_2^- = \dot{\theta}_3 \cos\theta_1^+ \cos\theta_2^+ - \dot{\theta}_3 \cos^2\theta_2^+$$

And for the assumption of the angles between hip and legs are all constant with  $90^\circ$ , there is extra torque at H.

We get the following compact equation between the pre-impact and post-impact angular velocities:

$$Q_-(\theta)\dot{\theta}^- = Q_+(\theta)\dot{\theta}^+$$

With matrices  $Q_-(\theta)$  and  $Q_+(\theta)$  given by:

$$Q_-(\theta) = \begin{pmatrix} -m_H \cos \theta_3^- \cos(\theta_1^- - \theta_2^-) & 0 & -m_H \cos \theta_1^- \sin \theta_2^- \sin \theta_3^- \\ m \cos \theta_3^- \cos(\theta_1^- - \theta_2^-) & -m \cos \theta_3^- & m \sin \theta_3^- \sin \theta_2^- (\cos \theta_1^- - \cos \theta_2^-) \\ 0 & 0 & -m_H \cos \theta_1^- \cos \theta_2^- \end{pmatrix}$$

$$Q_+(\theta) = \begin{pmatrix} m_H \cos \theta_3^+ + m \cos \theta_3^+ [1 - \cos(\theta_1^+ - \theta_2^+)] & m \cos \theta_3^+ [1 - \cos(\theta_1^+ - \theta_2^+)] \\ -m \cos \theta_3^+ \cos(\theta_1^+ - \theta_2^+) & m \cos \theta_3^+ \\ 0 & 0 \\ m_H \cos \theta_1^+ \sin \theta_1^+ \sin \theta_3^+ + m \sin \theta_3^+ [-\sin(\theta_1^+ + \theta_2^+) + \cos \theta_1^+ \sin \theta_1^+ + \cos \theta_2^+ \sin \theta_2^+] \\ m \sin \theta_3^+ \sin \theta_2^+ (\cos \theta_2^+ - \cos \theta_1^+) \\ -m_H \cos^2 \theta_1^+ - m(\cos \theta_1^+ - \cos \theta_2^+)^2 \end{pmatrix}$$

By doing the transition of the equation, we can avail the consequences of the model to the real robot model.

## 11. Conclusions and future work

The focus of the work is a relative further study of the passive gait of a compass-like, planar, biped robot with knees on inclined slopes. An analysis about the distribution of the energy and also the conversion law between the swing leg and the stance leg during the process of the steady robot gaits, have been discussed in the paper. Phase-position property corresponds to the limit cycle, the coupling properties between two legs, the existence of the culmination points which produced in the course of the conversion of KE and PE are also the topic of the research. To a certain slope angle  $\phi$ , one and only one stable limit cycle exists.

The research of the paper will have positive significance in getting better aware of the law and global property to biped gaits of the robot. The model we adopt here is quite applicable, how to enlarge the initial value attraction region of the limit cycle as well as how to apply the efficient control on the robot combined with its own property with the least energy possible will guide our further research direction.

## 12. Acknowledgement

This work is supported by the Research Fund for the Doctoral Program of Higher Education of China under grant 20090061120050 as well as the Forward and Crossing Research Fund for the Basic Theory in Jilin University under Grant 421033205410.

## 13. References

- [1] T. McGeer, "Passive dynamic walking", *International Journal of Robotics Research*, 9(2), pp. 62-82, 1990.
- [2] S.H. Collins, M. Wisse and A. Ruina, "A 3-d passive dynamic walking robot with two legs and knees", *International Journal of Robotics Research*, 20(7), pp. 607-615, 2001.
- [3] A. Goswami, B. Espiau and A. Keramane, "Limit cycles and their stability in a passive bipedal gait", *Proc. IEEE Conference on Robotics and Automation*, pp. 246-251, 1996.
- [4] M. Garcia, A. Chatterjee, A. Ruina and M. Coleman, "The simplest walking model: stability, complexity, and scaling", *ASME Journal of Biomechanical Engineering*, 120(2), pp. 281-288, 1998.
- [5] H. Ohta, M. Yamakita and K. Furuta, "From passive to active dynamic walking", *IEEE Conference on Decision and Control*, pp. 3883-3885, 1999.
- [6] A. Goswami, "Kinetic quantification of gait symmetry based on bilateral cyclograms", *Proc. XIXth Congress of the International Society of Biomechanics*, pp. 56-62, 2003.
- [7] A. Goswami, B. Thuilot and B. Espiau, "A study of the passive gait of a compass-like biped robot: symmetry and chaos", *International Journal of Robotics Research*, 17(12), pp. 1282-1301, 1998.
- [8] J.W. Grizzle, G. Abba and F. Plestan, "Asymptotically stable walking for biped robots: analysis via systems with impulsive effects", *IEEE Transactions on Robotics and Automation Control*, 46(1), pp. 51-64, 2001., pp. 51-64, 2001.
- [9] A. Goswami, B. Tuilot and B. Espiau, "Compass like bipedal robot part I: stability and bifurcation of passive gaits", *INRIA Research Report*, 1996.
- [10] G. Bhatia, M.W. Spong, "Hybrid control for smooth walking of a biped with knees and torso", *Proc. 2004 IEEE Conference on Control Applications*, pp. 88-96, 2004.
- [11] Y.F. Zheng, J. Shen, F.R. Sias, "A motion control scheme for a biped robot to climb sloping surfaces", *Proc. IEEE Conference on Robotics and Automation*, 2(4), pp. 814-816, 1988.
- [12] I. A. Hiskens, "Stability of hybrid system limit cycle: application to the compass gait biped robot", *Proceedings of 40th IEEE Conference on Decision and Control*, pp. 774-779, 2001.
- [13] A. Goswami, B. Tuilot and B. Espiau, "Compass like bipedal robot part I: stability and bifurcation of passive gaits", *INTRIA Research Report*, 1996.
- [14] M.W. Spong, G. Bhatia, "Further Results on Control of the Compass Gait Biped", *IEEE International Conference on Intelligent Robots and Systems Proceedings*, pp. 1933-1938, 2003.

- [15] M. Garcia, A. Chatterjee, A. Ruina and M. Coleman, "The simplest walking model: stability, complexity, and scaling", *ASME Journal of Biomechanical Engineering*, 120(2), pp. 281-288, 1998.

IntechOpen

IntechOpen



## **Biped Robots**

Edited by Prof. Armando Carlos Pina Filho

ISBN 978-953-307-216-6

Hard cover, 322 pages

**Publisher** InTech

**Published online** 04, February, 2011

**Published in print edition** February, 2011

Biped robots represent a very interesting research subject, with several particularities and scope topics, such as: mechanical design, gait simulation, patterns generation, kinematics, dynamics, equilibrium, stability, kinds of control, adaptability, biomechanics, cybernetics, and rehabilitation technologies. We have diverse problems related to these topics, making the study of biped robots a very complex subject, and many times the results of researches are not totally satisfactory. However, with scientific and technological advances, based on theoretical and experimental works, many researchers have collaborated in the evolution of the biped robots design, looking for to develop autonomous systems, as well as to help in rehabilitation technologies of human beings. Thus, this book intends to present some works related to the study of biped robots, developed by researchers worldwide.

### **How to reference**

In order to correctly reference this scholarly work, feel free to copy and paste the following:

Zhenze Liu, Yantao Tian and Changjiu Zhou (2011). Some Results on the Study of the Kneed Gait Biped, Biped Robots, Prof. Armando Carlos Pina Filho (Ed.), ISBN: 978-953-307-216-6, InTech, Available from: <http://www.intechopen.com/books/biped-robots/some-results-on-the-study-of-the-kneed-gait-biped>

**INTECH**  
open science | open minds

### **InTech Europe**

University Campus STeP Ri  
Slavka Krautzeka 83/A  
51000 Rijeka, Croatia  
Phone: +385 (51) 770 447  
Fax: +385 (51) 686 166  
[www.intechopen.com](http://www.intechopen.com)

### **InTech China**

Unit 405, Office Block, Hotel Equatorial Shanghai  
No.65, Yan An Road (West), Shanghai, 200040, China  
中国上海市延安西路65号上海国际贵都大饭店办公楼405单元  
Phone: +86-21-62489820  
Fax: +86-21-62489821

© 2011 The Author(s). Licensee IntechOpen. This chapter is distributed under the terms of the [Creative Commons Attribution-NonCommercial-ShareAlike-3.0 License](#), which permits use, distribution and reproduction for non-commercial purposes, provided the original is properly cited and derivative works building on this content are distributed under the same license.

IntechOpen

IntechOpen